Neodymium isotopic composition in foraminifera and authigenic phases of the South China Sea sediments: Implications for the hydrology of the North Pacific Ocean over the past 25 kyr

Qiong Wu, Christophe Colin, Zhifei Liu, François Thil, Quentin Dubois-Dauphin, Norbert Frank, Tachikawa Kazuyo, Louise Bordier, Eric Douville

AGU PUBLICATIONS

Geochemistry, Geophysics, Geosystems

RESEARCH ARTICLE
10.1002/2015GC005871

Key Points:
- εNd of foraminifera investigated for the first time in the South China Sea
- Improvement of the extraction of seawater Nd isotopes from marine sediments
- Past hydrological changes in the subtropical Pacific for the last 25 kyr

Correspondence to:
C. Colin,
christophe.colin@u-psud.fr

Citation:
Wu, Q., C. Colin, Z. Liu, F. Thil, Q. Dubois-Dauphin, N. Frank, K. Tachikawa, L. Bordier, and E. Douville (2015), Neodymium isotopic composition in foraminifera and authigenic phases of the South China Sea sediments: Implications for the hydrology of the North Pacific Ocean over the past 25 kyr, *Geochem. Geophys. Geosyst.*, *16*, 3883–3904, doi:10.1002/2015GC005871.

Received 27 APR 2015
Accepted 28 SEP 2015
Accepted article online 1 OCT 2015
Published online 11 NOV 2015

Neodymium isotopic composition in foraminifera and authigenic phases of the South China Sea sediments: Implications for the hydrology of the North Pacific Ocean over the past 25 kyr

Qiong Wu[1,2], Christophe Colin[2], Zhifei Liu[1], François Thil[3], Quentin Dubois-Dauphin[2], Norbert Frank[4], Kazuyo Tachikawa[5], Louise Bordier[3], and Eric Douville[3]

[1]State Key Laboratory of Marine Geology, Tongji University, 20092, Shanghai, China, [2]Laboratoire Geosciences Paris-Sud, UMR 8148, CNRS-Univ. Paris-Sud, Université Paris-Saclay, Orsay, France, [3]Laboratoire des Sciences du Climat et de l'Environnement, LSCE/IPSL, UMR 8212 CNRS-CEA-UVSQ, 91198, Gif-sur-Yvette, France, [4]Institute of Environmental Physics, Universität Heidelberg, Heidelberg, Germany, [5]Aix-Marseille Université, CNRS, IRD, CEREGE UM34, 13545, Aix en Provence, France

Abstract εNd and normalized Rare Earth Elements (REE) patterns of benthic and planktonic foraminifera and Fe-Mn coatings precipitated on sediments have been investigated for the South China Sea (SCS) to (1) assess the reliability of the extraction of past seawater εNd in the SCS and to (2) reconstruct past hydrological changes during the last 25 kyr. Reductively cleaned mono-specific planktonic foraminifera (*Globigerinoides ruber*) and mixed benthic foraminifera in core-top sediments from 1500 to 2400 m display similar εNd values to those of the modern Pacific Deep Water (PDW) (εNd of −3.9 to −4.4). Furthermore, the εNd of the reductive cleaning solutions shows similar εNd values to ones obtained on cleaned foraminifera. Combined with PAAS-normalized REE patterns, these results confirm that the oxidative and reductive cleaning procedure applied to foraminifera does not totally remove all of the Fe-Mn coatings and that εNd values yielded by cleaned planktonic foraminifera retain the εNd imprint of the bottom and/or pore water. εNd values obtained from a leaching procedure carried out on the bulk non-decarbonated sediments are comparable to the εNd values of the modern PDW, whereas a similar leaching procedure applied to decarbonated sediments reveals a bias due to contamination with Nd deriving from lithogenic particles. In core MD05-2904, seawater εNd, reconstructed from planktonic foraminifera, indicates that the last glacial period is characterized by lower εNd (−5.2 ± 0.2 to −6.4 ± 0.3) than the late Holocene (−4.1 ± 0.2). Assuming that Nd input from river does not change strongly the εNd of the PDW of the northern SCS, these εNd variations suggest a higher relative proportions of southern-sourced water in the deep water of the western subtropical Pacific Ocean during the last glacial period.

1. Introduction

The importance of global ocean circulation for climate variability is now widely recognized [*Broecker and Denton*, 1990; *Rahmstorf*, 2002]. The Pacific Ocean plays a key role in global ocean circulation in terms of heat redistribution through surface current flow from the equatorial areas to high latitudes, which in turn changes the carbon storage capacity of the ocean by deep water ventilation or stratification, resulting in significant climatic implications [*Matsumoto et al.*, 2002; *Herguera et al.*, 2010]. Even though it has received increasing attention over recent decades [*Talley and Joyce*, 1992; *Reid*, 1997; *Talley and Yun*, 2001; *Siedler et al.*, 2004; *Zenk et al.*, 2005; *Kawabe et al.*, 2003, 2005, 2006, 2009; *Kawabe and Fujio*, 2010], the evolution through time of North Pacific Deep Water and North Pacific Intermediate Water (NPDW and NPIW), as well as the penetration of southern-sourced water (SSW) into the North Pacific Ocean, is as yet not well constrained since the last glacial period and is still controversial [*Galbraith et al.*, 2007; *Okazaki et al.*, 2010; *Chikamoto et al.*, 2012; *Rella et al.*, 2012; *Jaccard and Galbraith*, 2013; *Max et al.*, 2014; *Rella and Uchida*, 2014].

The spatial distributions of the seawater neodymium (Nd) isotopic composition, expressed here as "$\varepsilon Nd = ([(^{143}Nd/^{144}Nd)sample/(^{143}Nd/^{144}Nd)_{CHUR}] - 1) \times 10{,}000$ (CHUR: Chrondritic Uniform Reservoir) [*Jacobsen and Wasserburg*, 1980]," have been recently established for the Philippine Sea and for the northern part of the SCS. This study highlights that seawater εNd of deep water masses in the Philippine Sea

results from the vertical mixing of the SSW, corresponding to the Upper Circumpolar Deep Water and Lower Circumpolar Deep Water (UCDW and LCDW) characterized by an εNd value of around −6 to −9 in the Southern Ocean [*Piepgras and Wasserburg*, 1982; *Jeandel*, 1993; *Carter et al*., 2012; *Amakawa et al*., 2013; *Stichel et al*., 2012; *Rickli et al*., 2014; *Basak et al*., 2015], and the northern-sourced water (NSW), corresponding to the North Pacific Deep Water and North Pacific Intermediate Water (NPDW and NPIW) characterized by εNd value of ∼−4 to −3 [*Piepgras and Jacobsen*, 1988; *Amakawa et al*., 2004, 2009]. In the deep ocean, the only way to alter the initial Nd isotopic composition of water mass is to add Nd with a different εNd values through riverine and eolian inputs and boundary exchange or by mixing isotopically different water masses [e.g., *Lacan and Jeandel*, 2001, 2005; *Goldstein and Hemming*, 2003; *Frank*, 2002]. The spatial distribution of seawater εNd in the northern SCS has shown that εNd of the deep water masses of the SCS below 1500 m is homogenous (−3.5 ± 0.3 and −4.5 ± 0.4) and similar to that of the deep Philippine Sea at similar and greater water depth (−3.6 ± 0.2 to −4.4 ± 0.4) [*Wu et al*., in press]. This implies that the εNd values of the PDW which enters the northern SCS through the Luzon Strait (>2400 m) is not modified by the exchange process [*Wu et al*., in press] and that Nd can be considered to faithfully trace water mass provenance and mixing of the Philippine Sea intermediate and deep water masses [*Wu et al*., in press].

Hence, seawater εNd record obtained from marine cores from the northwestern margin of the SCS can be considered to have a potential to assess the glacial-interglacial behavior of NSW and SSW in the North Pacific Ocean that has been debated. In this context, it is important to establish a reliable method for εNd extraction from the SCS marine cores. Recent studies have debated about how to extract seawater εNd signature from foraminifera and dispersed authigenic Fe-Mn coatings of deep-sea sediments [*Bayon et al*., 2002; *Vance et al*., 2004; *Piotrowski et al*., 2012; *Kraft et al*., 2013; *Tachikawa et al*., 2014]. While the Nd isotopic composition obtained from benthic foraminifera can be used to reconstruct bottom εNd seawater records, the significance of εNd values obtained from reductively and non-reductively cleaned planktonic foraminifera is still under debate [*Vance and Burton*, 1999; *Vance et al*., 2004; *Martínez-Botí et al*., 2009; *Kraft et al*., 2013; *Pena et al*., 2013; *Tachikawa et al*., 2013, 2014]. Investigation of REE in various phases of foraminifera suggests that approximately 90% of the REE reside in the coating fraction, and the remaining 10% is contained in the foraminifera calcite lattice [*Palmer*, 1985]. Thus, it has been proposed that εNd values obtained from the diagenetic Fe-Mn coatings precipitated on foraminiferal shells, primarily correspond to bottom seawater and/or pore water εNd values [*Tachikawa et al*., 2013, 2014]. Nevertheless, several other studies suggest that the reductive cleaning procedure can efficiently remove the Fe-Mn coatings precipitated on the planktonic foraminifera and can be used to establish εNd of surface or subsurface seawater [e.g., *Pena et al*., 2013; *Osborn et al*., 2008; *Martínez-Botí et al*., 2009].

The εNd seawater record for the late quaternary has been successfully reconstructed from εNd analyzed on the Fe-Mn oxide fraction leached from sediments collected in certain areas of the ocean [*Rutberg et al*., 2000; *Piotrowski et al*., 2004; *Gutjahr et al*., 2008; *Martin et al*., 2010]. In some other locations, however, especially close to continental margins under the influence of strong river discharges, εNd values of sediment leachates do not match the seawater εNd but appear to be biased by preformed Fe-Mn coatings delivered from rivers [*Bayon et al*., 2004; *Gutjahr et al*., 2008]. In addition, the analytical procedures permitting the correct extraction of seawater εNd from the authigenic phase in bulk sediments are controversial [*Bayon et al*., 2002; *Kraft et al*., 2013; *Piotrowski et al*., 2012]. Recently, *Wilson et al*. [2013] have reassessed the reliability of different approaches to extract Nd isotopes preserved in Fe-Mn coatings. These authors suggest that short leaching times and high sediment/solution ratios allow the extraction of seawater εNd from sediments and could be considered as a reliable proxy for reconstructing past seawater εNd. Nevertheless, the analytical procedure needs to be evaluated for each individual site rather than being used as a simple method that can be uniformly applied. In order to reconstruct past seawater εNd of the SCS, it is necessary to carefully verify that Nd isotopic compositions obtained from sediments and foraminifera are reliable and reflect seawater εNd signature. Here we have investigated several core-top samples from different parts of the SCS where a vertical gradient of the seawater εNd has been observed in order to evaluate the reliability of different procedures for the extraction of seawater εNd from foraminifera and Fe-Mn coatings of detrital particles. Nd values obtained from cleaned and uncleaned foraminifera are compared to seawater εNd recently measured by *Wu et al*. [in press]. Additionally, we present the Nd isotopic composition of foraminifera collected from sediments of a core located in the northern SCS to reconstruct the hydrology of the western subtropical North Pacific over the past 25 kyr.

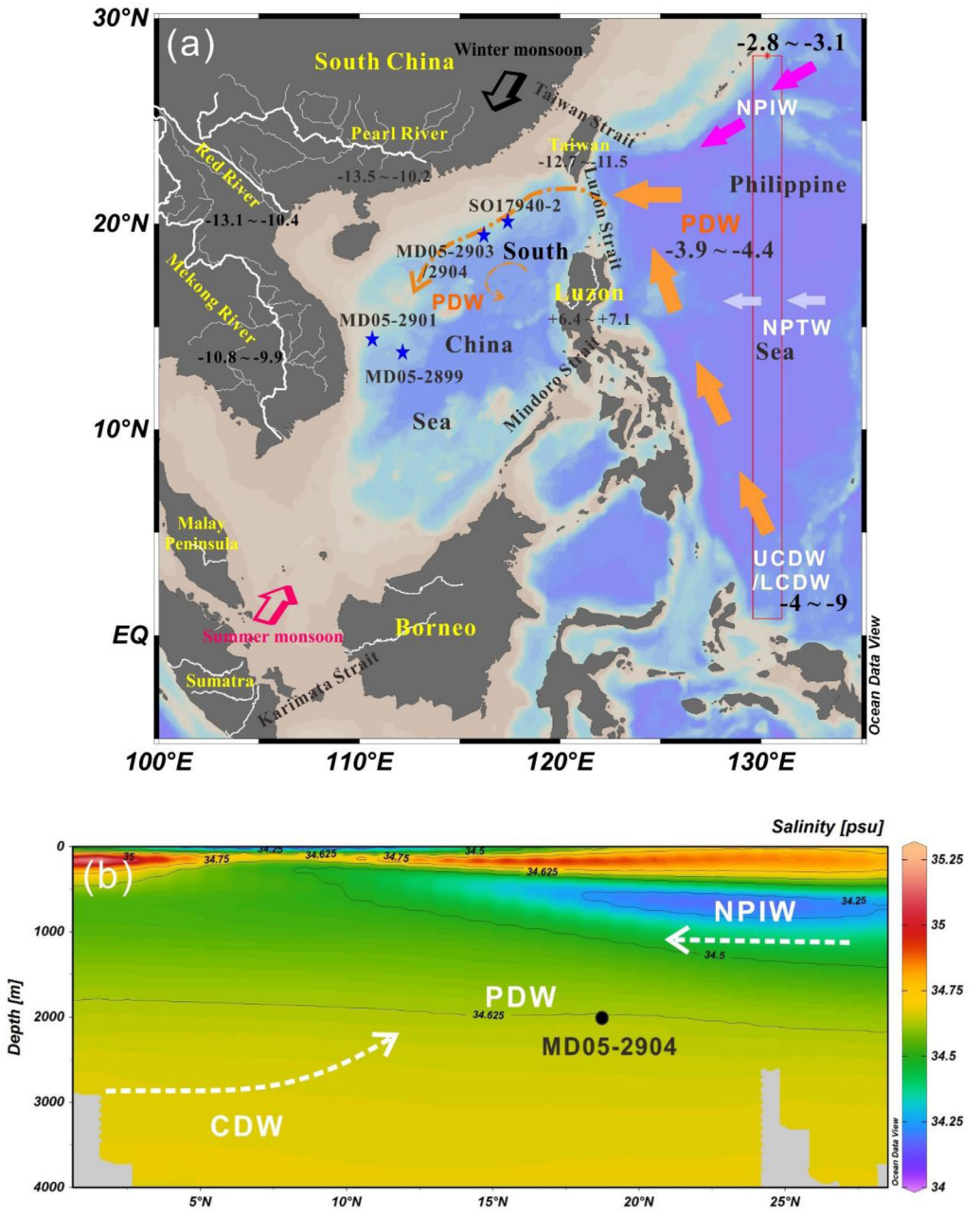

Figure 1. (a) Sample location map. The main deep water components in the Pacific Ocean have been also reported. LCDW: Lower Circumpolar Deep Water; UCDW: Upper Circumpolar Deep Water; PDW: Pacific Deep Water; NPIW: North Pacific Intermediate Water; NPTW: North Pacific Tropical Water. The εNd values of the main water masses have been also reported. Schematic deep water flow paths of CDW and NPIW are shown by orange and pink arrows, respectively. The NPTW has been shown in gray arrows. The orange dashed lines schematically denote the pathway of deep water flow from Philippine Sea to the SCS. (b) Latitudinal transect of annual mean salinity along the WOCE Pacific transect [*World Ocean Atlas*, 2013]). Core MD05-2904 is located in the PDW of the northern SCS that is characterized by similar hydrological parameter (T°C, S, and phosphate concentrations) [*Gong et al.*, 1992] to those of the WOCE Pacific transect reported in Figure 1b.

2. Hydrological Setting

The SCS is connected in the south with the Sulu and Java Seas through the shallow Mindoro (~200 m) and Karimata Straits (<50 m) and in the north with the East China Sea and Pacific Ocean through the Taiwan Strait (<100 m) and the deep channel of the Luzon Strait (>2400 m), respectively (Figure 1). Numerous studies have been undertaken of deep water circulation in the SCS (below 2000 m) in order to constrain the inflow and the pathway of the PDW into the SCS [*Li and Qu*, 2006; *Qu et al.*, 2006; *Wang et al.*, 2011; *Tian et al.*, 2006; *Zhao et al.*, 2014]. A vertical sandwich structure of water exchange between the SCS and the North Pacific has been

observed recently in the Luzon Strait that is the only deep connection between the SCS and the North Pacific. During the winter, an inflow of western Pacific water into the SCS occurs in the surface and deep layers while an outflow to the Philippine Sea can be observed at intermediate depth compensating for inflow [*Gong et al*., 1992; *Tian et al*., 2006]. Water masses below 2000 m in the SCS are characterized by relatively homogenous physical properties (2.1–2.3°C, 34.59–34.62) similar to those of the PDW observed in the Philippine Sea at around 2000 m [*Li and Qu*, 2006; *Qu et al*., 2006; *World Ocean Atlas Data*, 2013]. The PDW, characterized by a low temperature (1.6°C) and high salinity (34.62), sinks in the deep SCS basins immediately after it crosses the Luzon Strait [*Wyrtki*, 1961]. It enhances the vertical mixing (upwelling) and potentially contributes to the upper layer circulation [*Tian et al*., 2009; *Li and Qu*, 2006; *Qu et al*., 2006; *Qu*, 2002]. These processes facilitate the rapid turnover of the SCS deep water that has been recently estimated at around 30–70 years [*Qu et al*., 2006; *Chang et al*., 2010]. The basin-scale oxygen distribution suggests that deep water which enters the SCS is transported north-westward to the northern slope of the SCS and thereafter southward along the western margin of the sea (Figure 1) [*Qu et al*., 2006; *Li and Qu*, 2006]. The South China Sea Intermediate Water (SCSIW) (350–1350 m) is characterized by higher salinity than the NPIW observed in the Philippine Sea. This is due to vertical diffusion of the SCSIW with deep water in the SCS [*Chen et al*., 2001; *Xie et al*., 2011; *Tian et al*., 2009]. The intrusion of NPIW has been found to be greater in winter than in summer and is associated with leakage of the Kuroshio Current [*Qu et al*., 2006; *Chen and Huang*, 1996]. Mid-depth water exchange in the Luzon Strait also displays seasonal variability. During the winter, there is an inflow of the NPIW into the SCS through the southern part of the Luzon Strait whereas the outflow of the SCSIW to the Philippine Sea is located in the northern part of the Luzon Strait. These water masses flow in an opposite direction during the summer [*Tian et al*., 2006; *Yang et al*., 2010; *Xie et al*., 2011].

Above a depth of 350 m, surface and subsurface circulations in the SCS are mainly controlled by the seasonal reversals of the wind direction during the summer and winter monsoons. This induces a cyclonic surface circulation in winter and an anticyclonic one in summer [*Shaw and Chao*, 1994; *Fang et al*., 1998]. The surface North Pacific Tropical Water (NPTW), characterized by high salinity, enters the SCS and is diluted by freshwater discharged by the large Asian rivers, thereby inducing the relatively fresher South China Sea Tropical Water (SCSTW) [*Xie et al*., 2011].

More recently, *Wu et al*. [in press] showed that below 2000 m εNd values of deep water masses of the Philippine Sea and the northwestern margin of the SCS present a narrow range between -3.5 ± 0.3 and -4.5 ± 0.4, corresponding to the presence of the PDW. In the Philippine Sea, above a depth of around 1000 m, the NPIW is characterized by εNd values that reach -2.7 ± 0.4 and which are similar to those obtained from the subtropical North Pacific. εNd of the SCSIW is slightly lower (between -3.6 ± 0.3 and -3.9 ± 0.3) than that of the NPIW due to vertical diffusion with the PDW in the SCS [*Wu et al*., in press].

3. Material and Methods

3.1. Material

The Calypso cores MD05-2899 (13°47.66′N, 112°10.89′E, 2393 m), MD05-2901 (14°22.503′N, 110°44.6′E, 1454 m), MD05-2903 (19°27.31′N, 116°15.06′E, 2047 m), and MD05-2904 (19°27.32′N, 116°15.15′E, 2066 m) were retrieved on the northwestern margin of the SCS during the R/V Marion Dufresne MARCO POLO IMAGES XII Cruise in 2005 (Figure 1 and Table 1).

Four core-top sediments were sampled from each core where Holocene sediments are well identified by preliminary δ^{18}O curves obtained on planktonic foraminifera (unpublished data). These core-top sediments were investigated to represent modern time or at least late Holocene. In addition, seven additional downcore sediment samples were collected in the upper 10 m of core MD05-2904. The age model of core MD05-2904 has been first established by *Ge et al*. [2010] and modified by *Wan and Jian* [2014]. It is based on 16 C-14 AMS dates obtained from planktonic foraminifera *G. ruber*. On the basis of age model, the eight downcore sediment samples provide snapshots on hydrological conditions of the northern SCS spanning the last 25 kyr (Table 1).

3.2. Analytical Procedures

Thirty milligram of mono-specific planktonic foraminifera *G. ruber*, mixed planktonic foraminifera, and around 8 mg mixed benthic foraminifera, with shell sizes larger than 150 μm, were handpicked under a

Table 1. Nd Isotopic Composition, Nd/Ca and Mn/Ca Ratios of Reductively Cleaned Foraminifera and Cleaning Solutions[a]

Core/Station	Latitude	Longitude	Water Depth (m)	Age (kyr)	Sample ID	εNd	2σ	Mn/Ca (μmol/mol)	Nd/Ca (μmol/mol)
MD05-2903	19.45°N	116.25°E	2047	Core top	Cleaned *G. ruber*	−4.7	0.2		
				Core top	Cleaned BF	−3.7	0.4		
				Core top	Cleaning solution of *G. ruber*	−4.3	0.4		
				Core top	Cleaning solution of BF	−4.7	0.4		
MD05-2901	14.28°N	110.74°E	1454	Core top	Cleaned *G. ruber*	−6.3	0.3		
				Core top	Cleaned BF	−6.9	0.2		
				Core top	Cleaning solution of *G. ruber*	−7.2	0.2		
				Core top	Cleaning solution of BF	−6.9	0.4		
MD05-2899	13.79°N	112.19°E	2393	Core top	Cleaned *G. ruber*	−6.6	0.2		
				Core top	Cleaned BF	−5.9	0.3		
				Core top	Cleaning solution of *G. ruber*	−6.2	0.4		
				Core top	Cleaning solution of BF	−6.0	0.4		
MD05-2904	19.46°N	116.25°E	2066	0.14	Cleaned *G. ruber*	−4.1	0.2	216	1.12
				0.14	Cleaning solution of *G. ruber*	−4.1	0.3		
				0.14	Cleaned BF	−4.1	0.4	295	1.98
				0.14	Cleaning solution of BF	−4.8	0.4		
MD05-2904	19.46°N	116.25°E	2066	0.14	Cleaned foraminiferas of mixed species	−4.2	0.3	128	0.62
MD05-2904	19.46°N	116.25°E	2066	0.14	Uncleaned *G. ruber*	−4.2	0.2	613	1.74
MD05-2904	19.46°N	116.25°E	2066	2.13	Cleaned *G. ruber*	−4.4	0.3	139	0.79
MD05-2904	19.46°N	116.25°E	2066	2.13	Cleaning solution of *G. ruber*	−4.2	0.3		
MD05-2904	19.46°N	116.25°E	2066	6.25	Cleaned *G. ruber*	−4.7	0.2	298	1.37
MD05-2904	19.46°N	116.25°E	2066	6.25	Cleaning solution of *G. ruber*	−5.0	0.3		
MD05-2904	19.46°N	116.25°E	2066	6.25	Cleaned BF	−4.2	0.5	338	1.38
MD05-2904	19.46°N	116.25°E	2066	6.25	Uncleaned *G. ruber*	−4.8	0.2	859	1.78
MD05-2904	19.46°N	116.25°E	2066	11.18	Cleaned *G. ruber*	−5.1	0.2	421	1.16
MD05-2904	19.46°N	116.25°E	2066	11.18	Uncleaned *G. ruber*	−5.2	0.2	837	1.74
MD05-2904	19.46°N	116.25°E	2066	15.25	Cleaned *G. ruber*	−6.2	0.3	278	0.90
MD05-2904	19.46°N	116.25°E	2066	15.25	Cleaning solution of *G. ruber*	−6.4	0.3		
MD05-2904	19.46°N	116.25°E	2066	19.17	Cleaned *G. ruber*	−6.4	0.3	182	0.77
MD05-2904	19.46°N	116.25°E	2066	19.17	Cleaning solution of *G. ruber*	−6.1	0.3		
MD05-2904	19.46°N	116.25°E	2066	20.80	Cleaned *G. ruber*	−5.9	0.2	301	1.49
MD05-2904	19.46°N	116.25°E	2066	20.80	Cleaning solution of *G. ruber*	−5.6	0.3		
MD05-2904	19.46°N	116.25°E	2066	20.80	Cleaned foraminiferas of mixed species	−5.9	0.3	190	1.60
MD05-2904	19.46°N	116.25°E	2066	22.45	Cleaned *G. ruber*	−5.6	0.2	375	1.72
MD05-2904	19.46°N	116.25°E	2066	22.45	Cleaning solution of *G. ruber*	−5.2	0.3		
St8 (D3)	20°2.9′N	117°25′E	5		Seawater	−3.3	0.4		
St8 (D3)	20°2.9′N	117°25′E	2000		Seawater	−4.2	0.4		
St11 (10-JJW-82)	18°30′N	114°15′E	5		Seawater	−5.3	0.4		
St11 (10-JJW-82)	18°30′N	114°15′E	2000		Seawater	−3.5	0.3		
St13 (SEATS)	17°59′N	115°59′E	5		Seawater	−7.0	0.3		
St13 (SEATS)	17°59′N	115°59′E	2000		Seawater	−3.6	0.3		
St15 (10-JJW-55)	14°31′N	111°00′E	5		Seawater	−8.5	0.3		
St16 (10-JJW-46)	11°00′N	111°00′E	5		Seawater	−7.1	0.3		

[a] εNd values from seawater samples obtained from *Wu et al.* [in press] have been also reported for comparisons.

binocular microscope. All of the foraminifera were gently crushed between two glass plates to open all chambers. The calcite fragments were then ultrasonicated for 1 min before pipetting the suspended particles with water to separate the waste. This step was repeated until the water became clear and free of clay. All samples were checked under a binocular microscope to ensure that all particles had been removed. Physically cleaned samples were transferred to centrifuge tubes for the oxidative-reductive cleaning step (foraminifera which underwent this process are hereafter referred to as "cleaned foraminifera"). For the purpose of comparison, three samples were subjected to mechanical cleaning only (hereafter referred to "uncleaned foraminifera"). The oxidative-reductive foraminiferal cleaning procedure used in this study followed that described by *Vance and Burton* [1999], using 10 mL reductive solution (1 *M* hydrous hydrazine, 16 *M* NH_4OH, 0.25 *M* citric acid + 16 *M* NH_4OH in a ratio of 1:6:3) and 5 ml oxidative solution (0.2 *M* NaOH and 30% H_2O_2 in a 1:1 ratio) per sample to more efficiently remove authigenic Fe-Mn coatings. For the reductive step, samples were heated in a water bath at 80°C for 30 min and were ultrasonicated every 2.5 min for 10 s. After transferring the reductive cleaning solution to a centrifuge tube, the cleaned foraminifera were rinsed with Milli-Q water. The analytical procedure for the oxidative step was similar except that samples were ultrasonicated every 10 min for a period of 30 s. All samples, including non-reductively cleaned samples, underwent a weak acid leaching for 5 min in 1 ml 0.001 *M* HNO_3 with ultrasonication. After the

cleaning step, samples were transferred into a 1.5 ml tube. A 0.5 ml of deionized water was first added to the tube, and then the foraminifera were dissolved using stepwise 100 μl nitric acid (0.5 *M* HNO_3) until the dissolution reaction stopped. The dissolved samples were centrifuged and the supernatant was immediately transferred to Teflon beakers to prevent the leaching of any possible remaining phases. All of the dissolved foraminifera shell fraction and authigenic fraction contained in the reductive cleaning solution were dried using a hotplate for Nd purification. Element concentrations and REE patterns analysis were performed on a 10% cut of both the dissolved foraminifera shells and the corresponding reductive cleaning solutions collected from core MD05-2904.

Several studies have been carried out to test the reliability of seawater-derived Nd extraction from bulk sediments involving different leaching procedures [*Bayon et al*., 2002; *Gutjahr et al*., 2007; *Wilson et al*., 2013; *Molina-Kescher et al*., 2014b]. First, it is recommended to not remove the carbonate fraction of the bulk sediments; second, the leaching time should not be too long; third, the sample size/leachate ratios need to be large [*Wilson et al*., 2013]. In this study, in order to better constrain the reliability of using bulk sediments leachates to reconstruct past seawater εNd from sediments of the northern SCS, an evaluation was conducted on five samples covering the Holocene and the Last Glacial Maximum (LGM). First, sequential analysis was performed on ground samples of 0.2, 1, and 2 g which were simply rinsed with deionized water and then directly leached with 7 ml 0.02 *M* hydroxylamine hydrochloride in 25% (v/v) acetic acid (HH solution) for 30 min. Then, five additional samples of 1 g were treated using the same leaching procedure but with a longer leaching time of 1 h. Parallel 1 g samples of sediment were decarbonated using a sodium acetate buffered acetic acid solution, and subjected to 30 min of leaching with 7 mL 0.02 *M* HH solution in order to assess the possible influence of the decarbonation process. Decarbonated samples of 0.2 g were leached for 30 min, 2 h, and 3 h with 0.02 *M* HH solution in order to test the influence of leaching times.

Nd was purified from all samples following the analytical procedure described in detail by *Copard et al*. [2010]. In brief, we used TRU-Spec and Ln-Spec resins following the method described in detail by *Pin and Santos Zalduegui* [1997]. In this method, samples were loaded using 2 ml of 1 *M* HNO_3 on preconditioned TRU-Spec columns (83 mg portion of TRU-spec). The unwanted cations were eluted using five portions of 0.5 ml of 1 *M* HNO_3. The TRU-Spec columns were then placed over the Ln-Spec columns. The light REE were then eluted from the upper (TRU-Spec) column using seven portions of 0.1 ml of 0.05 *M* HNO_3. After decoupling from the TRU-Spec columns, La, Ce, and most of the Pr were removed from the Ln-Spec columns using 3.25 ml of 0.25 *M* HCl. Nd was then eluted with an additional 2.5 ml of 0.25 *M* HCl.

3.3. Ca, Mn, and REE Concentrations and $^{143}Nd/^{144}Nd$ Analysis

Ca, Mn, and REE concentrations were determined at the Laboratoire des Sciences du Climat et de l'Environnement (LSCE) by measuring their isotopes ^{44}Ca, ^{55}Mn, and ^{146}Nd using a Thermo Scientific Inductively Coupled Plasma-Quadrupole Mass Spectrometer (ICP-QMS X Series^{II}). The used protocol, previously described by *Bourdin et al*. [2011], is briefly described as follows. Carbonate sample and standard solutions were systematically adjusted to 100 ppm Ca through dilution. This is because (1) high Ca levels need to be avoided as high contents can increase salt deposition on cones and consequently affect ICP-QMS stability and (2) adjusted Ca concentration levels introduced into ICP-QMS at 100 μl/min provide a way to control matrix effects due to the presence of Ca. Instrumental calibration, based on the standard addition method, was achieved using multielementary standard solutions. The signal drift through the analytical sessions was monitored and corrected by the analysis every nine samples of blank and carbonate standard JCp-1 solutions. Other carbonate standards (JCt-1, ARAG-AK, BAM, and GSR-6) were also regularly analyzed to validate elemental concentrations. When analyzing the REE of the reductive cleaning solution from foraminifera and leachates from bulk sediments, a high-purity REE solution was also measured and additional internal standards (^{115}In and ^{103}Rh) were added to sample and standard solutions. Our measurements were characterized by analytical uncertainties ranging from 5% for the lightest REE to 15% for the heaviest [*Bourdin et al*., 2011]. The reproducibility of measurements for two repeated samples varied according to the different element to calcium ratios (2σ: 10% for Mn/Ca, 5% for Nd/Ca). The Nd concentrations in blanks are systemically lower than 0.1 ppb, which is negligible compared to the average concentration of 15 ppb ± 5% measured in samples.

The $^{143}Nd/^{144}Nd$ ratios were analyzed using the Thermo Fisher Neptune^{Plus} Multi-collector Inductively Coupled Plasma Mass Spectrometer (MC-ICP-MS) at the Laboratoire des Sciences du Climat et de l'Environnement (LSCE) in Gif-sur-Yvette. The Nd isotopic composition was analyzed at a concentration of 10–15

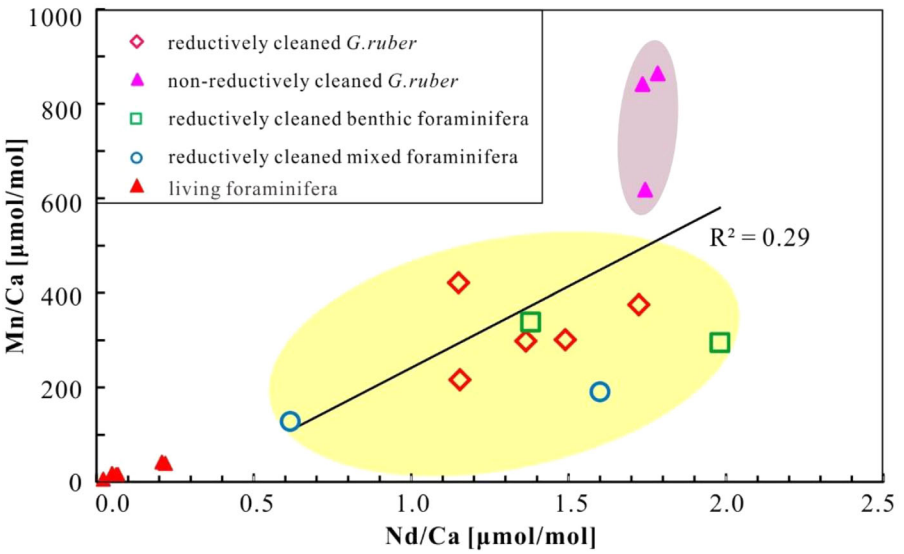

Figure 2. Mn/Ca ratios versus Nd/Ca ratios obtained on reductively cleaned and non-reductively cleaned foraminifera samples (planktonic foraminifera *G. ruber*, benthic foraminifera, and mixed foraminifera) of core MD05-2904. Non-reductively cleaned foraminifera show higher Mn/Ca ratios compared to reductively cleaned foraminifera. Mn/Ca and Nd/Ca ratios obtained from *Pomiès et al*. [2002] for living foraminifera have been reported for comparison.

ppb. The mass-fractionation correction was made by normalizing $^{146}Nd/^{144}Nd$ to 0.7219 and applying an exponential-fractionation correction. During the analytical sessions, every two samples were bracketed with analyses of appropriate Nd standard solutions JNdi-1 and La Jolla characterized by certified values of 0.512115 ± 0.000006 [*Tanaka et al*., 2000] and 0.511858 ± 0.000007 [*Lugmair et al*., 1983], respectively. Standard solutions JNdi-1 and La Jolla were analyzed at concentrations similar to those of the samples and we have corrected all of the measurements affected by a machine bias when necessary by using the La Jolla standard. The external reproducibility (2σ) for time resolved measurement, deduced from repeated measurements of the La Jolla standard and JNdi-1, ranged from 0.2 to 0.4 Epsilon units for various analytical sessions. The analytical error associated to each sample analysis is taken as the external reproducibility of the La Jolla standard for each session. Blank values were $<$100 pg and can be neglected as they represent less than 1% of the sample Nd analyzed.

4. Results

4.1. Element/Ca Ratios and REE Concentrations

Ca, Mn, and REE concentrations were measured on dissolved cleaned foraminifera and reductive cleaning solutions in order to evaluate the efficiency of the cleaning procedures. Mn/Ca ratios range from 128 to 421 µmol/mol for cleaned foraminifera and from 613 to 859 µmol/mol for uncleaned foraminifera (Figure 2 and Table 1). Unlike Mn/Ca ratios, Nd/Ca ratios in cleaned foraminifera are randomly distributed from 1.12 to 1.72 μmol/mol, with one exception with very low ratios (0.62 μmol/mol). Nd/Ca ratios obtained from uncleaned foraminifera are around 1.74–1.78 μmol/mol. Although the uncleaned foraminifera are characterized by higher Mn/Ca ratios, Nd/Ca ratios in cleaned and uncleaned foraminifera display similar ranges of level and are not correlated with Mn/Ca ratios ($r^2 = 0.29$) (Figure 2).

REE concentrations obtained from planktonic and benthic foraminifera and reductive cleaning solutions were normalized to Post-Archean Average Australian Shales (PAAS) [*Nance and Taylor*, 1976]. All of the PAAS-normalized REE patterns are quite similar and present no or pronounced negative Ce anomalies as well as Middle REE (MREE) enrichment (Figure 3a). This pattern with a negative Ce anomaly, especially for low REE concentration samples, is similar to other published seawater REE patterns in the SCS [*Alibo and Nozaki*, 2000]. PAAS-normalized REE of reductive cleaning solution shows a clear MREE enrichment (Figure 3b).

REE concentrations were also measured in leachates obtained from bulk non-decarbonated and decarbonated sediments. The PAAS-normalized REE patterns display a MREE enrichment that is independent of the leaching procedures (Figure 4). For bulk non-decarbonated core-top samples (Figures 4a–4d), the REE

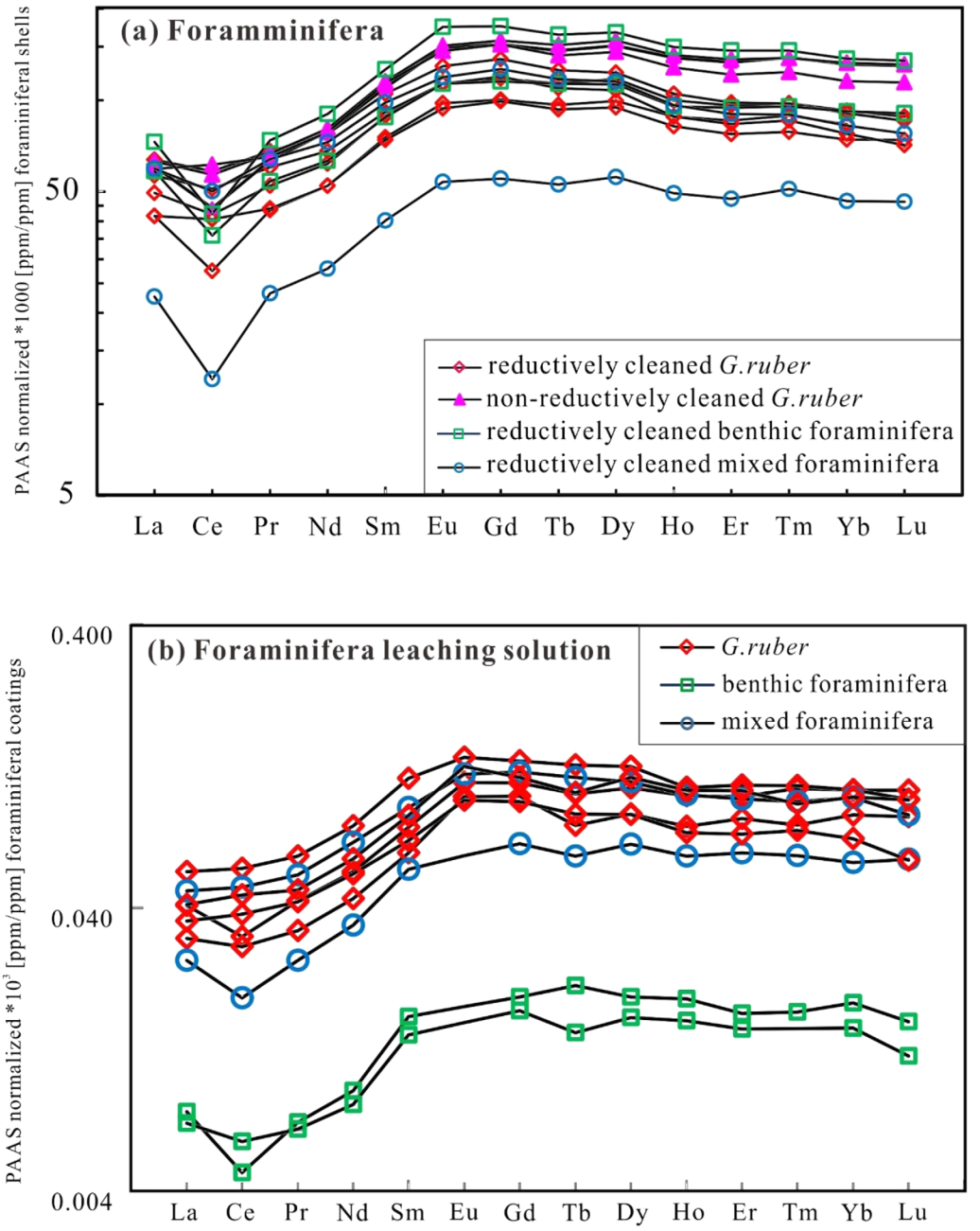

Figure 3. (a) PAAS-normalized REE patterns obtained on reductively cleaned and non-reductively cleaned foraminifera samples of core MD05-2904 (planktonic foraminifera *G. ruber*, benthic foraminifera, and mixed foraminifera); (b) PAAS-normalized REE patterns obtained from reductive cleaning solutions.

patterns show moderate negative Ce anomalies regardless of the sample sizes and leaching time. The downcore samples of core MD05-2904 do not present negative Ce anomalies. Leachates of all the decarbonated samples exhibit MREE enrichment with no negative Ce anomalies (Figures 4e–4h).

4.2. εNd in Foraminifera and Bulk Sediments Leachates

εNd values obtained on mono-specific samples of planktonic foraminifera *G. ruber*, mixed planktonic foraminifera, and mixed benthic foraminifera lie in a narrow range from -3.7 ± 0.4 to -4.7 ± 0.4 for the core-top sample from MD05-2903 and from -4.1 ± 0.2 to -4.8 ± 0.4 for the core-top sample from MD05-2904 (Table 1). It is worth noting that mean εNd values obtained on foraminifera cleaning solutions are similar or weakly more unradiogenic. εNd values for all foraminifera samples and reductive cleaning solutions from

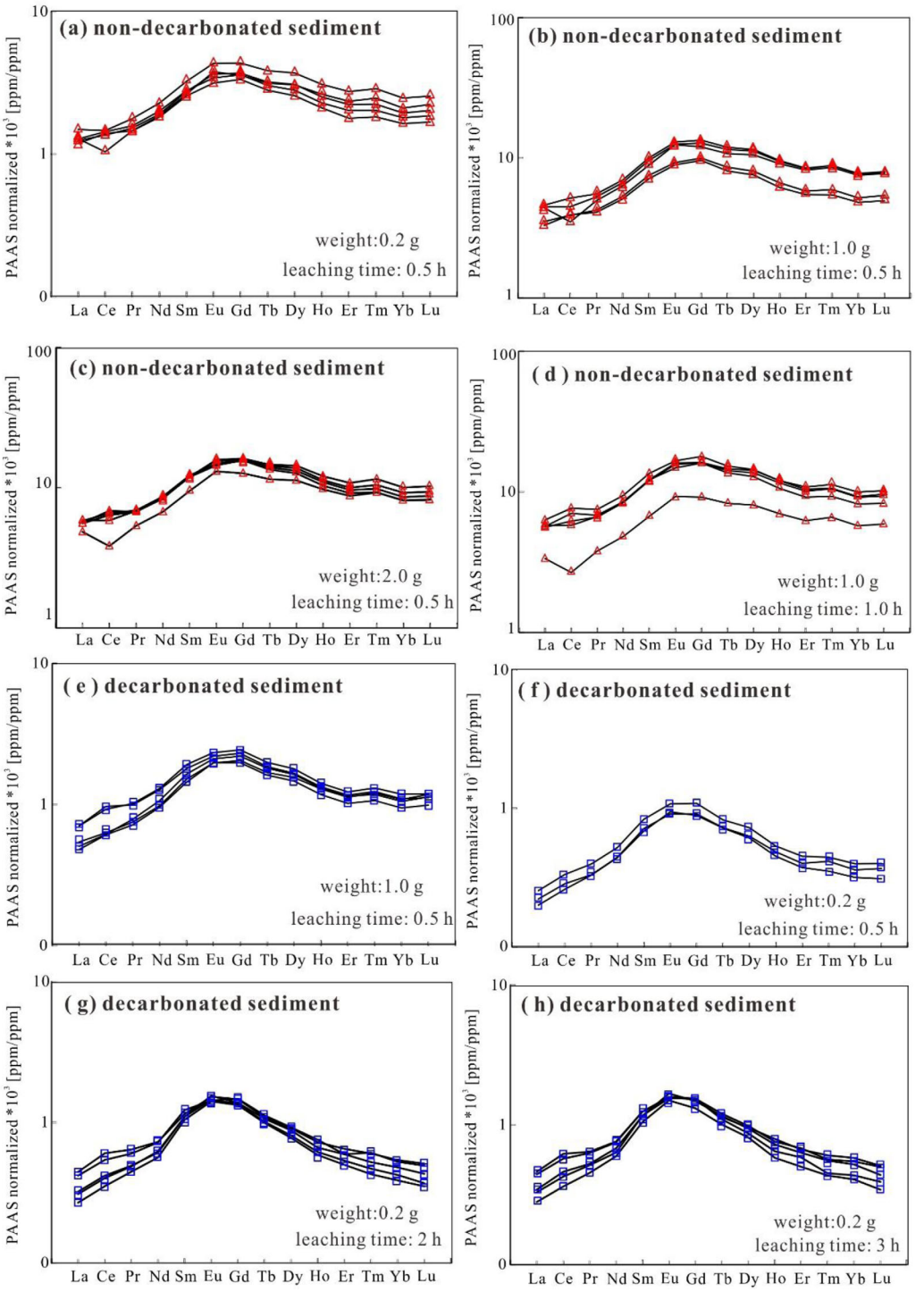

Figure 4. PAAS-normalized REE patterns obtained from sediment leachate solutions of downcore samples from core MD05-2904. (a–d) Results obtained on different size of bulk non-decarbonated sediments (0.2, 1, and 2 g) and different time of leaching (0.5 and 1 h); (e–h) results obtained on different size of decarbonated sediments (0.2 and 1 g) and different time of leaching (0.5, 2, and 3 h).

core-top samples of cores MD05-2899 and MD05-2901 (obtained from a more southern position of the SCS), ranged from -5.9 ± 0.3 to -6.6 ± 0.2, and from -6.3 ± 0.3 to -7.2 ± 0.2, respectively. Consequently, εNd values obtained on the same sediment sample from a mono-specific sample of planktonic foraminifer *G. ruber*, mixed planktonic foraminifera, mixed benthic foraminifera, and reductive cleaning solution are more or less in the same range (Table 1) and each core-top sediments shows specific εNd values.

In core MD05-2904, εNd values were analyzed on samples of foraminifera from the Holocene and the late last glacial period. εNd values of all samples of foraminifera investigated from core MD05-2904 exhibited a wide range from -6.4 ± 0.3 to -4.1 ± 0.2 (Table 1 and Figure 5). The late glacial period is characterized, on average, by lower εNd (-5.2 ± 0.3 to -6.4 ± 0.3) than the late Holocene (-4.1 ± 0.2). In general, εNd values obtained for each mono-specific sample of planktonic foraminifera *G. ruber*, mixed planktonic foraminifera, mixed benthic foraminifera, and from the reductive cleaning solution are in agreement within uncertainty (Figure 5b).

For core MD05-2904, εNd obtained from HH leachates of decarbonated and non-decarbonated sediments are outlined in Figure 6b and Table 2. εNd obtained from HH leachates of bulk non-decarbonated sediments vary from -6.4 ± 0.3 for glacial sediments to -4.4 ± 0.3 for core-top samples. On the other hand, εNd obtained from leachates of decarbonated sediments range from -7.0 ± 0.2 for glacial sediments to -5.5 ± 0.3 for core-top samples and average values for each age studied here systematically display lower εNd of around 1.0 Epsilon unit compared to non-decarbonated sediments. For both non-decarbonated and decarbonated sediments, εNd values are slightly affected by the leaching procedure used in this study. In general, an increase in the leaching time (from 0.5 to 3 h) and a reduction of sample weight (from 1 to 0.2 g) is associated to a significant decrease of the εNd values (Figure 6 and Table 2).

5. Discussion

5.1. Elemental Ratios and REE Patterns in Foraminifera

The Mn/Ca ratio in foraminifera has been identified as an indicator for early diagenetic Fe-Mn oxides, or Mn-rich carbonates, which precipitated on the foraminiferal carbonate [*Boyle*, 1983; *Pomiès et al*., 2002]. The ratio is usually used to monitor the efficiency of reductive cleaning [*Boyle*, 1983; *Pena et al*., 2005]. Mn/Ca ratios in the reductively cleaned foraminifera shells (128–421 μmol/mol) are around 3 times lower than those of the non-reductively cleaned foraminifera samples (613–859 μmol/mol). However, such values are 10–30 times higher than Mn/Ca ratios obtained from living and nonfossil planktonic foraminifera collected in plankton tows and sediment traps (0.25–15 μmol/mol) [*Pomiès et al*., 2002; *Martínez-Botí et al*., 2009; *Roberts et al*., 2012]. Similarly, Nd/Ca ratios from cleaned foraminifera (1.15–1.72 μmol/mol) are much higher than Nd/Ca ratios obtained previously from planktonic foraminifera collected in sediment traps (0.008–0.70 μmol/mol) [*Pomiès et al*., 2002; *Martínez-Botí et al*., 2009] (Figure 2).

Whereas Nd/Ca ratios in both reductively cleaned and uncleaned foraminifera exhibit different values, no linearly decreasing trend from uncleaned samples to cleaned samples was observed (Figure 2). However, all reductively cleaned foraminifera (*G. ruber*, benthic or mixed foraminifera) tend to reveal a weak link between Nd/Ca and Mn/Ca ratios in foraminifera ($r^2 = 0.29$). *Palmer* [1985] has suggested that around 90% of REE were incorporated into authigenic phases in foraminifera shell. In addition, the distribution of planktonic foraminifera Nd investigated recently at micrometer scale has revealed that Nd concentration in Fe-Mn-rich parts was much higher than in foraminiferal calcite, where Nd distribution was randomly heterogeneous [*Roberts et al*., 2012; *Tachikawa et al*., 2013]. The weak link between Nd/Ca and Mn/Ca ratios of cleaned foraminifera observed in our study might also imply that the cleaning procedure used do not totally remove all the Fe-Mn coatings and Nd carried by these authigenic phases. Reductively and non-reductively cleaned foraminifera exhibit similar REE patterns with a moderate to negative Ce anomaly and a MREE enrichment similar to those identified in dissolved foraminifera and fossil fish teeth [*Gutjahr et al*., 2007; *Martin et al*., 2010; *Kraft et al*., 2013]. REE patterns in both the surface and deep water in the SCS [*Wu et al*., in press], and in other ocean basins, merely display pronounced negative Ce anomaly but no MREE enrichment (Figure 4) [*Alibo and Nozaki*, 2000; *Bayon et al*., 2011; *Jeandel et al*., 2013]. Several hypotheses have been put forward to explain this puzzling feature [*Palmer*, 1985; *Elderfield et al*., 1990; *Hannigan and Sholkovitz*, 2001; *Haley et al*., 2005]. In general, these authors hypothesize that the MREE enrichment in various dissolved phases is related to fractionated REE incorporated in foraminifera or more truly an overprinted pore water signature during early diagenetic processes. Authigenic phases in marine sediments were suggested to be an important carrier of REE as they contain higher concentrations of REE than foraminiferal tests [*Piotrowski et al*., 2012; *Roberts et al*., 2012; *Tachikawa et al*., 2013]. REE patterns characterized by MREE enrichment have been observed in both pore water and Fe-Mn hydroxide phases [*Haley et al*., 2004; *Surya Prakash et al*., 2012]. Here PAAS-normalized REE patterns obtained from cleaned foraminifera and

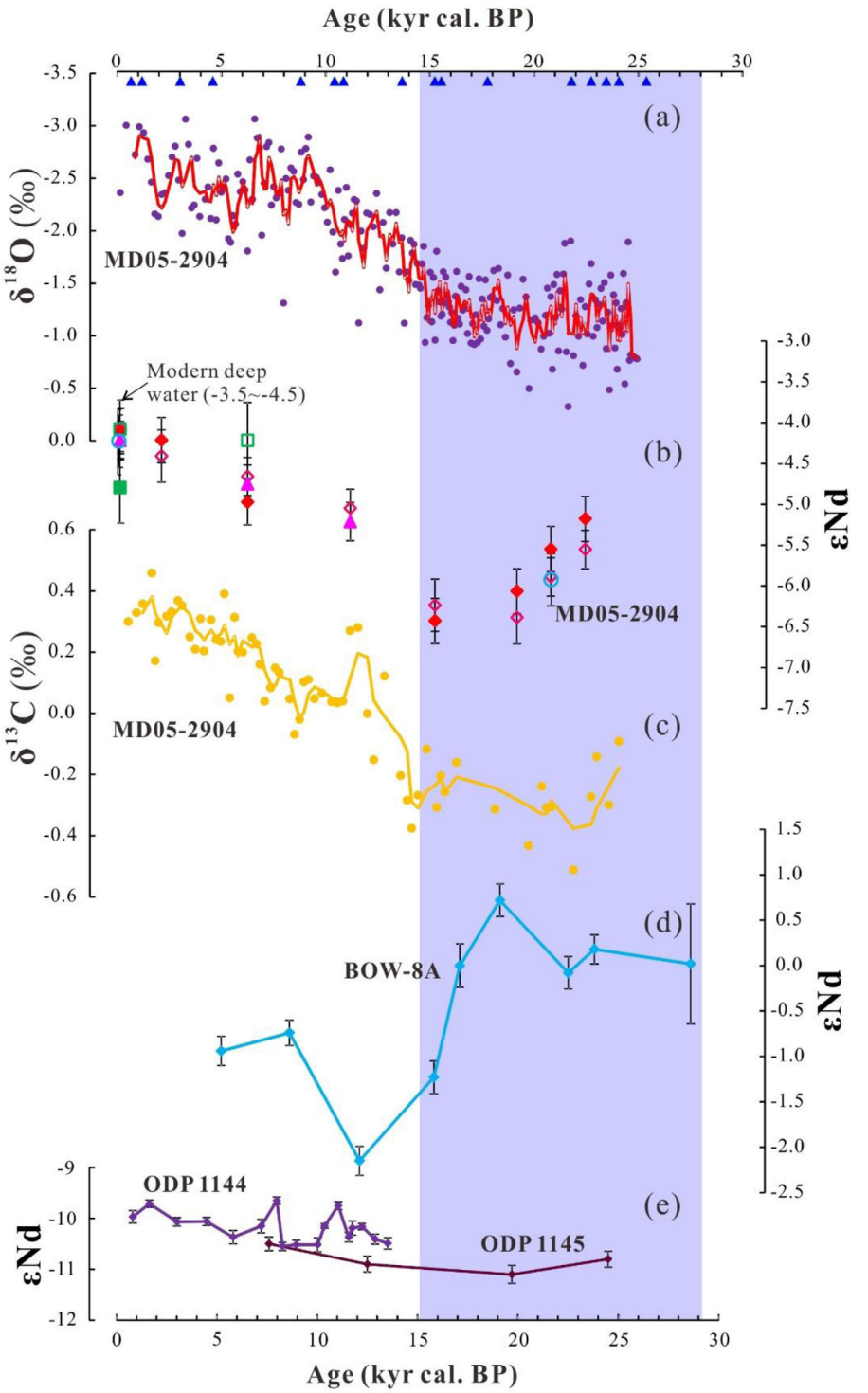

Figure 5. (a) δ^{18}O records obtained from planktonic foraminifera *G. ruber* of core MD05-2904 over the past 25 kyr [*Ge et al.*, 2010; *Wan and Jian*, 2014]; smooth curve is derived from a three-point average result (red line). Blue triangles show AMS ^{14}C age control points [*Ge et al.*, 2010; *Wan and Jian*, 2014]; (b) εNd values obtained from cleaning solution of *G. ruber* (solid red diamond), reductively cleaned *G. ruber* (empty pink diamond), non-reductively cleaned *G. ruber* (solid pink triangle), reductively cleaned mixed foraminifera (empty light blue circle), reductively cleaned benthic foraminifera (empty green rectangle), and cleaning solution of benthic foraminifera (solid green rectangle). εNd values of water masses at the similar water depth of core MD05-2904 (2000 m) are reported for comparison; (c) δ^{13}C records obtained from benthic foraminifera *C. wuellerstorfi* of core MD05-2904 [*Wan and Jian*, 2014]. (d) εNd records obtained from the authigenic fraction of sediments from core BOW-8A located in the Bering Sea (54°47′N, 176°55′E, 884 m) [*Horikawa et al.*, 2010]; (e) εNd of the decarbonated-fraction of sediments from the ODP Sites 1144 (20°3.180′, 117°25.133′, 2035 m) and 1145 (19°35.040′, 117°37.868′, 3175 m) [*Boulay et al.*, 2005; *Hu et al.*, 2012].

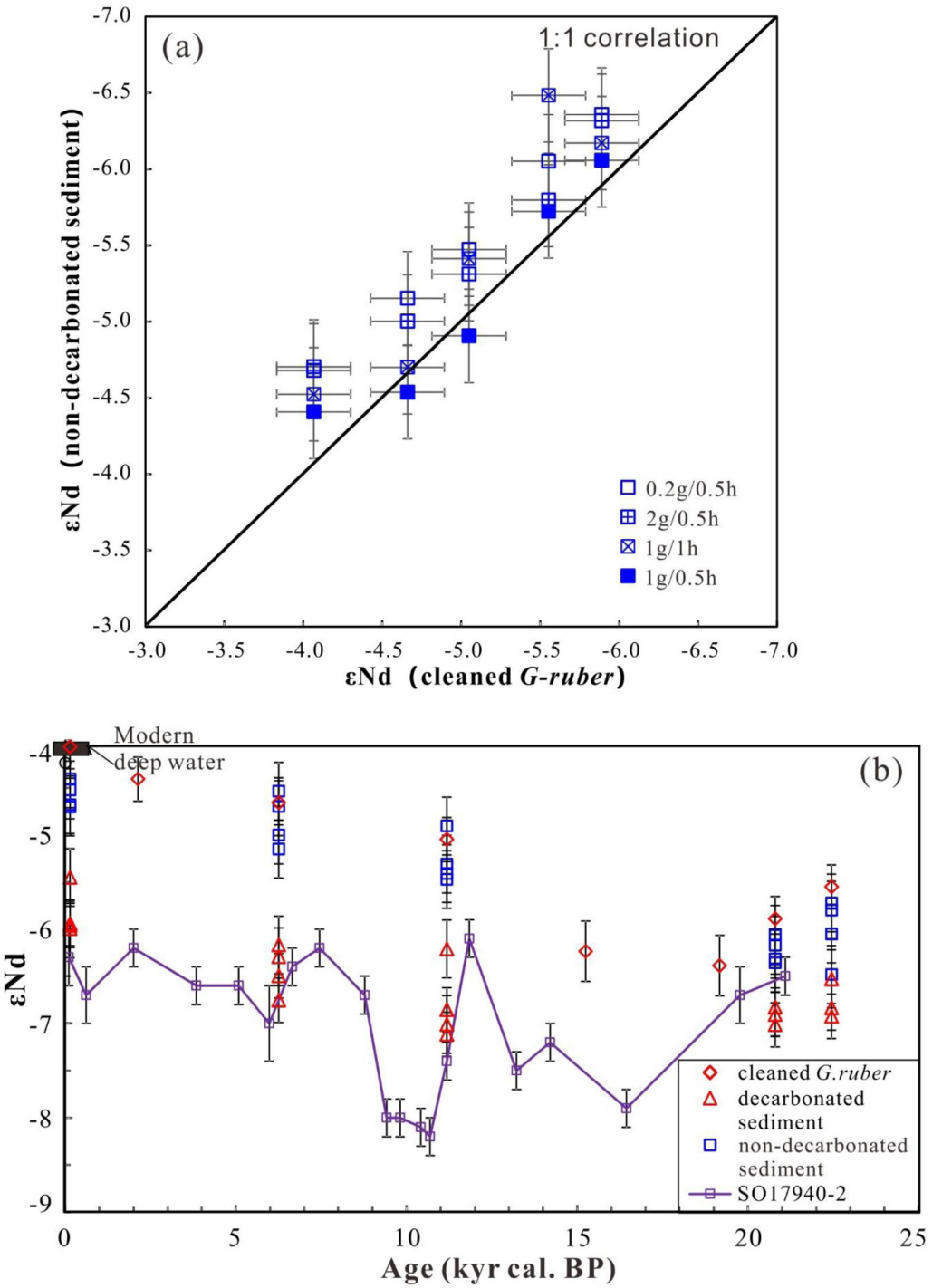

Figure 6. (a) Crossplot of εNd values of non-decarbonated sediment leachates and εNd values obtained from cleaned planktonic foraminifera *G. ruber*. (b) εNd values obtained from acid-reductive HH leachates of bulk non-decarbonated and decarbonated sediments of core MD05-2904. εNd values have been obtained by using HH leaching of 0.2, 1, and 2 g samples of sediments leached for 0.5, 1, 2, and 3 h. εNd obtained on seawater samples close to the studied site [*Wu et al.*, in press] as well on cleaned planktonic foraminifera *G. ruber* of core MD05-2904 are also reported. εNd from acid-reductive HH leachates of bulk decarbonated sediments of the core SO17940-2 [*Huang et al.*, 2013] are also reported for comparison.

reductive cleaning solutions are similar (Figures 3a and 3b). Thus, we suggest that MREE enrichment in foraminifera is associated with REE incorporated in authigenic components precipitated on the foraminifera. For the reductive cleaning solutions, PAAS-normalized REE patterns are similar to those of foraminifera shells (Figures 3a and 3b). It can be noted that both cleaned benthic foraminifera (two samples from core

Table 2. Nd Isotopic Composition of Bulk Sediment Leachates Measured Along the Gravity Core MD05-2904[a]

Sed. Age (kyr)	Carbonate Treatment	Weight (g)	Leaching Time (min)	εNd	2σ	εNd (Average)
0.14	Non-decarbonated	0.20	30	−4.7	0.3	−4.6
	Non-decarbonated	1.00	30	−4.4	0.3	
	Non-decarbonated	2.00	30	−4.7	0.3	
	Non-decarbonated	1.00	60	−4.5	0.3	
	Decarbonated	0.20	30	−6.0	0.3	−5.9
	Decarbonated	0.20	120	−6.0	0.2	
	Decarbonated	0.20	180	−6.0	0.2	
	Decarbonated	1.00	30	−5.5	0.3	
6.25	Non-decarbonated	0.20	30	−5.2	0.3	−4.9
	Non-decarbonated	1.00	30	−4.5	0.3	
	Non-decarbonated	2.00	30	−5.0	0.3	
	Non-decarbonated	1.00	60	−4.7	0.3	
	Decarbonated	0.20	30	−6.0	0.3	−6.4
	Decarbonated	0.20	120	−6.5	0.2	
	Decarbonated	0.20	180	−6.8	0.2	
	Decarbonated	1.00	30	−6.2	0.3	
11.18	Non-decarbonated	0.20	30	−5.5	0.3	−5.3
	Non-decarbonated	1.00	30	−4.9	0.3	
	Non-decarbonated	2.00	30	−5.4	0.3	
	Non-decarbonated	1.00	60	−5.3	0.3	
	Decarbonated	0.20	30	−7.1	0.3	−6.8
	Decarbonated	0.20	120	−6.9	0.2	
	Decarbonated	0.20	180	−7.1	0.2	
	Decarbonated	1.00	30	−6.2	0.3	
20.80	Non-decarbonated	0.20	30	−6.4	0.3	−6.2
	Non-decarbonated	1.00	30	−6.1	0.3	
	Non-decarbonated	2.00	30	−6.2	0.3	
	Non-decarbonated	1.00	60	−6.1	0.3	
	Decarbonated	0.20	120	−6.9	0.2	−6.9
	Decarbonated	0.20	180	−7.0	0.2	
	Decarbonated	1.00	30	−6.8	0.3	
22.45	Non-decarbonated	0.20	30	−6.1	0.3	−6.1
	Non-decarbonated	1.00	30	−5.7	0.3	
	Non-decarbonated	2.00	30	−5.8	0.3	
	Non-decarbonated	1.00	60	−6.5	0.3	
	Decarbonated	0.20	120	−6.9	0.2	−6.7
	Decarbonated	0.20	180	−6.8	0.2	
	Decarbonated	1.00	30	−6.5	0.3	

[a]^{14}C ages were published by *Ge et al*. [2010] and *Wan and Jian* [2014].

MD05-2904) and corresponding coating solutions are characterized by slightly lower concentrations in REE and exhibit marked negative Ce anomalies typical of the seawater (Figure 3). This may be due to a less contribution of authigenic phases to REE contents in these benthic foraminifera. In addition, εNd obtained from the reductive cleaning solution is characterized by slightly more negative value (−4.8) compared to the cleaned foraminifera (−4.2), thus suggesting the influence of a small contribution of lithogenic particulate reactivity (εNd = −12).

In summary, we observed here that the chemical cleaning process could not fully remove the Nd related to authigenic phases. Therefore, εNd values obtained in both reductively cleaned and non-reductively cleaned planktonic foraminifera are more likely to be associated with bottom and/or pore water εNd values rather than surface seawater values, being consistent with a recent review [*Tachikawa et al*., 2014].

5.2. REE Patterns in Bulk Sediment Leachate

PAAS-normalized REE patterns of leachates obtained from bulk sediments display MREE enrichment regardless of leaching procedures (Figures 4a–4d), indicating significant contribution of REE from Fe-Mn hydroxides [*Haley et al*., 2005; *Bau and Koschinsky*, 2009]. Previous studies have shown that a long leaching time could introduce REE contamination from lithogenic fraction thereby leading to unusual Ce anomalies [*Bayon et al*., 2002; *Gutjahr et al*., 2007]. In this study, using identical leaching times, core-top samples display a negative Ce anomaly whereas anomaly was absent for downcore samples (Figures 4a–4d). Moreover, leachates from decarbonated sediments did not display a negative Ce anomaly. Thus, the leaching time

does not seem to be a main factor influencing detrital contribution. REE mobilization has been reported during the early state of diagenesis associated with redox cycling of Fe-Mn oxyhydroxides within surface sediment leading to preferential Ce enrichment in pore water [*Elderfield and Sholkovitz*, 1987]. Several studies show positive Ce anomalies associated with Fe-Mn oxide after leaching of the easily exchangeable fraction of ferromanganese deposits [*Ohta and Kawabe*, 2001; *Bau and Koschinsky*, 2009]. Hence, we suggest that the positive Ce anomalies in some samples here that did not undergo carbonate removal might be due to REE remobilization during the early diagenitic process and that the presence of carbonate could reduce REE extraction from detrital fraction thus avoiding contamination by the residue. Alternatively, decarbonation partially attacks detrital phase, which facilitates REE release from terrigenous fraction.

5.3. εNd in the Foraminifera and Reductive Cleaning Solutions of Core-Top Samples

εNd values determined from cleaned mono-specific samples of planktonic foraminifera (*G. ruber*), cleaned mixed foraminifera, nonreductively cleaned planktonic foraminifera, mixed benthic foraminifera, and associated authigenic phases, all taken from core-top samples from the same site, are characterized by a narrow range (Table 1 and Figure 5).

εNd values obtained from core-top samples exhibit variations of at least 2 Epsilon units between the northern and the western middle part of the SCS (Table 1). For cores MD05-2904 and MD05-2903, located in the northern SCS, εNd values varied from -4.1 ± 0.2 to -4.8 ± 0.4 and from -3.7 ± 0.4 to -4.7 ± 0.4, respectively. Seawater εNd values at the surface and at depth of both cores obtained from neighboring water stations are reported in Table 1. Benthic and planktonic foraminifera and their associated authigenic phases are similar to those of the deep water of the northern SCS (εNd between $\sim -4.2 \pm 0.4$ to -3.5 ± 0.3; Table 1) and are significantly different from surface seawater samples ($\sim -7.0 \pm 0.3$ to -5.3 ± 0.4). For cores MD05-2899 and MD05-2901 in the western middle part of the SCS, εNd values varied from -5.9 ± 0.3 to -6.6 ± 0.2 and from -6.3 ± 0.3 to -7.2 ± 0.2, respectively. Although εNd values from deep water are not available for the southern and middle part of the SCS, the reported proximal surface water εNd are more negative ($\sim -8.5 \pm 0.3$ to -7.1 ± 0.3) compared with the εNd values observed in foraminifera and incorporated authigenic phases [*Amakawa et al*., 2000; *Wu et al*., in press] (Table 1). These results confirm that εNd obtained from planktonic foraminifera do not exhibit the imprint of the surface seawater εNd. Taking into consideration that planktonic and benthic foraminifera yield similar εNd values for each of the cores investigated, we can hypothesize that foraminifera have recorded the εNd from bottom water and confirm that the Nd isotopic composition of foraminifera is mainly marked by εNd of authigenic phases as shown by Nd/Ca and Mn/Ca ratios and PAAS-normalized REE patterns. Such results support recent studies [*Pomiès et al*., 2002; *Elmore et al*., 2011; *Kraft et al*., 2013; *Tachikawa et al*., 2013] suggesting that foraminifera record the Nd isotopic seawater composition of the bottom water. It implies also that seawater εNd values below 1500 m of the western middle part of the SCS are characterized by slightly more negative values than those of the northern SCS, possibly due to the influence of local sources [*Wu et al*., in press]. Further investigations need to be carried out in the future on seawater εNd of the southern SCS to verify such hypothesis.

5.4. Nd Isotopic Composition Discrepancy in Bulk Sediment Leachates for the Last 25 kyr

In core MD05-2904, εNd values obtained from foraminifera samples from the Holocene and the Last Glacial Maximum (LGM) exhibited a large range from -6.4 ± 0.4 to -4.1 ± 0.2 (Figure 5 and Table 1). The LGM period is characterized on average by more unradiogenic εNd (-5.2 ± 0.3 to -6.4 ± 0.4) than the late Holocene (-4.1 ± 0.2). In general, εNd values obtained from mono-specific samples of planktonic foraminifera *G. ruber*, mixed planktonic foraminifera, and mixed benthic foraminifera are similar and suggest that significant changes of seawater εNd have taken place over the past 25 kyr in the northern SCS.

εNd values obtained from HH leachates of bulk non-decarbonated sediments from the same core-top samples (MD05-2904), extracted by using different leaching procedures, range from -4.4 ± 0.3 to -4.7 ± 0.3 and are similar to modern seawater εNd in the northern SCS at a depth of about 2000 m (between -3.5 ± 0.3 and -4.5 ± 0.4) [*Wu et al*., in press]. In addition, there is a good agreement between HH leachates of bulk non-decarbonated sediments and εNd obtained from foraminifera (Figure 6a). For all of the samples that we have investigated, HH leachates of non-decarbonated sediments of 1 g, leached for 0.5 h, yields εNd values closest to those obtained from cleaned *G. ruber* (Figure 6a and Table 2). The results indicate that seawater εNd could be extracted by this leaching procedure for bulk non-decarbonated sediments from our study site.

In contrast, εNd values obtained from decarbonated sediments from the core-top samples (−5.5 ± 0.3 to −6.0 ± 0.2) differ from those of deep water in the northern SCS (−3.5 ± 0.3 to −4.5 ± 0.3) [*Wu et al*., in press] (Figure 6b and Table 2). For each sample investigated in core MD05-2904, the εNd values obtained from the decarbonated sediments systematically display values 1.5 Epsilon units lower than non-decarbonated sediments or cleaned *G. ruber*. Such offset in the εNd values are also observed even if the best condition of HH leaching determined on non-decarbonated sediments (1 g of sample with 0.5 h leaching time) is applied.

For the purposes of comparison, the results of *Huang et al*. [2013], who extracted εNd from acid-reductive HH leachates of decarbonated sediments of the core SO17940-2 (20°07.0′N, 117°23.0′E; water depth of 1727 m) bathed in similar water mass to core MD05-2904, are reported in Figure 6b. The εNd record core SO17940-2 do not show glacial-interglacial changes and εNd values obtained on the core-top samples (−6.3 ± 0.3) is not consistent with the εNd range of PDW analyzed in the SCS at same water depth (−4.0 to −4.5). The εNd record of this core is systematically more unradiogenic than the εNd derived from foraminifera in our study but it is similar to the values obtained from core MD05-2904 using a similar leaching procedure on the decarbonated sediment fraction (0.2 g of sample with 2 h leaching time).

Considering that detrital material of surface sediments around the study sites MD05-2904 and SO17940-2 are characterized by an εNd of about −11 [*Wei et al*., 2012; *Liu et al*., 2015], the negative offset observed in εNd from HH leachates of decarbonated sediments may be caused by Nd deriving from the lithogenic fraction during the leaching procedure. Nevertheless, the εNd record obtained by *Huang et al*. [2013] is probably a mixing between lithogenic Nd extracted by the analytical procedure used and seawater εNd variability that might explain why both εNd records display quite similar variations particularly between 25 and 15 kyr. The contamination of εNd from lithogenic fraction, volcanic ash, and/or preformed Fe-Mn oxides has already been discussed in several studies [*Bayon et al*., 2002; *Elmore et al*., 2011; *Wilson et al*., 2013; *Kraft et al*., 2013]. All of these results support the idea that removing carbonate may promote dissolution of detrital fraction. In contrast, HH leachates of non-decarbonated sediments from the SCS provide bottom water εNd under certain sample size/solution ratios and leaching times, in agreement with results recently obtained in the Indian Ocean [*Wilson et al*., 2013].

5.5. Hydrological Implications for the Pacific Since the LGM

The large range of εNd values obtained from foraminifera from core MD05-2904 (between −6.4 ± 0.4 and −4.1 ± 0.2) reflects major changes in the seawater εNd during the last 25 kyr (Figure 5b). To understand such εNd variations, it is necessary to determine the εNd of the water masses circulating in the northern SCS or, at least, to identify the main potential isotopic mixing end-members involved in the water mass balance. One must also take into account that the Nd isotopic composition of these end-members could be changed since the last glacial period.

The spatial distribution of present seawater εNd has recently been established for the Philippine Sea and the northern SCS permitting the identification of the εNd of the main water masses of the SCS and the Philippine Sea. Results show a homogenous Nd isotopic composition for the PDW throughout the northern SCS, similar to the Nd isotopic composition of the PDW in the Philippine Sea (∼−4) [*Wu et al*., in press]. Any significant modification of the εNd value of the PDW was detected after it enters the SCS implying a negligible role for the "boundary exchange" process in the northern SCS [*Wu et al*., in press].

The seawater εNd on the northwestern margin of the SCS seem to be not strongly influenced by "boundary exchange" [*Lacan and Jeandel*, 2001, 2005] since the last glacial period because εNd values of sediments from the northwestern margin of the SCS have not changed drastically over the past 25 kyr. The sedimentary sources along this oceanic margin correspond mainly to the Pearl River and Taiwanese Rivers, which are characterized by similar ranges of εNd from −10.2 to −13.5 and from −11.5 to −12.7, respectively [*Liu et al*., 2007; *Wei et al*., 2012]. A small contribution of lithogenic material deriving from the volcanic arc of Luzon (mainly smectite), transported by surface and intermediate currents, has been also identified in sediments on the northwestern margin of the SCS [*Boulay et al*., 2005; *Liu et al*., 2010]. However, the εNd distribution of detrital material of surface sediment in the northern SCS presents a narrow value range (from −11 to −12) [*Wei et al*., 2012] implying a strong dilution of the volcanic material by sediments deriving from Taiwanese and Chinese Rivers. Over the last 25 kyr B.P., changes in εNd of the detrital fraction of the ODP Sites 1144 and 1145, located close to core MD05-2904, are only between −9.9 and −11.1 [*Boulay et al*., 2005; *Hu et al*., 2012] (Figure 5e)

that is insufficient to explain the 2 Epsilon Nd unit variations observed in the reconstructed seawater εNd record obtained from core MD05-2904 (Figure 5b). However, the quantity of sediments transfers to the north-western margin of the SCS since the last glacial period could be also modified by changes of Asian summer monsoon rainfall intensity and by the reworking of the shelf's sediment during low sea level stand [e.g., *Boulay et al*., 2005]. These processes have the potential to modify sediments transport to the deep water basin and the dissolved Nd input from the Pearl River to the studied site. However, at present days, εNd values of the PDW along the northwestern margin of the SCS is not modified in nepheloide layers as well as in different part of the northern SCS characterized by contrasted terrigenous fluxes environment [*Wu et al.*, in press]. In addition, εNd record obtained in core MD05-2904 at low time resolution display a significant decrease of εNd values between 23 and 15 ka and an increase of εNd values during the last glacial-interglacial transition until about 7 ka that are not related to any major changes of the shoreline and river month position induce by sea level variations. Nevertheless, past seawater εNd record from the north-western margin of the SCS need to be investigated at a higher time resolution in the further investigation to assess any potential impacts of variations sea level and sediments transfer to the deep basin on the Nd budget of the SCS.

In addition, the modern SCS deep water refresh very rapidly with a resident time estimated between 30 and 70 years [*Qu et al*., 2006; *Chang et al*., 2010]. Further, potential change in bottom water residence time in the north-western SCS during LGM might have only negligible effect on seawater εNd variability because dissolved-particulate interaction is estimated to be very quick (from weeks to months [*Jeandel and Oelkers*, 2015]).

Consequently, assuming that the Nd budget of the northern SCS is not strongly modified since the last glacial time, the large variations of bottom water εNd values between the LGM (-6.4 ± 0.2) and the Holocene (-4.1 ± 0.2) estimated for core MD05-2904 could be interpreted as indicating a major re-organization of intermediate/deep water circulation in the Pacific during the last deglaciation and/or a major changes of the Nd isotopic composition of water masses (Figure 5b).

With the exception of εNd values obtained in the Northwest Pacific close to the East China Sea that have been interpreted as being the result of lithogenic input, εNd values of the modern NPDW, obtained from several water stations in the North Pacific, are generally characterized by radiogenic values of ~ -4 [*Piepgras and Wasserburg*, 1980; *Amakawa et al*., 2004, 2009]. The εNd of the glacial NPDW is actually not available. However, in the Bering Sea, *Horikawa et al*. [2010] have shown that εNd obtained from the authigenic fraction of sediments from core BOW-8A (54°47′N, 176°55′E, 884 m) displays more radiogenic values (+0.8) during glacial time than the Holocene (−2) (Figure 5d). This has been interpreted as being the result of enhanced vertical mixing of the NPIW with surface water displaying a high radiogenic Nd isotopic composition strongly influenced by sediment from the volcanic margin of the Bering Sea (Aleutian Arc and Kamchatka Peninsula) [*Horikawa et al*., 2010]. Such variations in the εNd of the NPIW observed in the subarctic region would have had a remarkable influence, through vertical mixing, on the Nd isotopic signature of the glacial NPDW and would have produced a more radiogenic glacial NPDW in the North Pacific. In addition, during glacial times, it has been shown by modeling and various proxies such as ventilation age changes that glacial NPDW could be produced in different areas of the North Pacific [*Okazaki et al*., 2010; *Rae et al*., 2014]. However, as seawater εNd of the upper layer of the North Pacific range from ~ -2.8 to -4.5 [*Amakawa et al*., 2004, 2009], the glacial NPDW need to stay through time a radiogenic end-member and cannot explain the negative εNd values of the glacial seawater obtained from core MD05-2904.

Present-day εNd values of AAIW and CDW (SSW) in the south Pacific range from -6 to -8.5 and from -8 to -9 [*Molina-Kescher et al*., 2014a; *Carter et al*., 2012; *Amakawa et al*., 2013]. The SSW and particularly the AAIW are strongly modified in the North Pacific by dilution with NPDW and NPIW [*Piepgras and Jacobsen*, 1988] and by boundary exchange or exchange with volcanic particulates derived from numerous volcanic areas [*Amakawa et al*., 2009; *Grenier et al*., 2013]. The εNd values of the SSW during glacial periods is poorly constrain but a shift toward more radiogenic values was identified during the HS1 for the AAIW in cold-water corals (~ -6.5) of the Drake Passage [*Robinson and van de Flierdt*, 2009] and during the LGM for deep-sea cores collected at different water depth from the Chatham Rise (continental slope basin East of New Zealand) [*Noble et al*., 2013]. This study indicates a glacial LCDW εNd of around -5.6 corresponding to an offset up to ∼0.8 εNd-units more radiogenic than those obtained for glacial deep water on core MD05-2904 (-5.2 ± 0.3 to -6.4 ± 0.3) and for South Atlantic and equatorial Indian ($\varepsilon Nd = -6.4$ to -7.4) [*Piotrowski et al*., 2004, 2009]. However, as seawater εNd at the Chatham Rise are influenced by the signature of the NPDW and could be modified locally by boundary exchange or exchange with volcanic particles derived

from New Zealand's North Island, further investigations are necessary to constrain the Nd isotopic composition of the glacial UCDW and LCDW. Nevertheless, the glacial εNd values of the SSW (AAIW and CDW) in the southern Pacific is less radiogenic compared to the Holocene of about more than 1 εNd-units reflecting a reduced export of NADW due to re-organization of the Atlantic meridional overturning circulation, which was propagated throughout the glacial Southern Ocean [*Piotrowski et al*., 2004, 2009]. The modification of the CDW in the North Pacific by boundary exchange or exchange with volcanic particulates derived from numerous volcanic areas has been observed for surface and intermediate water masses [*Grenier et al*., 2013], but are not well documented for deep water masses of the southern Philippine Sea that could contribute significantly to the upper layer by vertical mixing. The modifications of the εNd values of the glacial CDW during northward penetration are also not available for the LGM.

Nevertheless, assuming that the glacial CDW (−7) was not fully modified from the Southern Ocean to the Philippine Sea during the last glacial period, the seawater εNd record obtained from core MD05-2904 could reflect a modification of the proportions of the NSW (NPIW/NPDW) and the SSW (CDW) in the Philippine Sea (Figure 5b). The LGM, characterized by unradiogenic εNd values compared to those of the Holocene, would imply a retreat of the NSW (NPIW/NPDW) to the north and/or a higher propagation of the SSW (CDW) to the north compared to the modern situation, which is characteristic of the late Holocene period (last 6 kyr) (Figure 5b). Such interpretation needs to be confirmed by further investigation of εNd record in the western equatorial Pacific to determine the Nd isotopic composition of the glacial CDW in the southern Philippine Sea.

Previous studies have suggested that NPIW formation was more intense during the last glacial period [*Rella et al*., 2012; *Max et al*., 2014] or during the cold event HS1 in the subarctic Pacific [*Okazaki et al*., 2010; *Chikamoto et al*., 2012; *Jaccard and Galbraith*, 2013]. According to compilation of radiocarbon records in the North Pacific combined with modeling simulation, it has been suggested that the formation of NPIW could even extend to a depth of 3600 m [*Okazaki et al*., 2010; *Rae et al*., 2014]. The simulated deep water pathways spread southward along the western margin of the North Pacific, forming a simple western boundary deep current system that can reach the Philippine Sea and the northern SCS [*Okazaki et al*., 2010; *Wan and Jian*, 2014].

However, such a scenario, implying a higher proportion of NSW during the LGM, is not supported by the seawater εNd record from core MD05-2904 that in contrast implies a higher proportion of SSW (Figure 5b). It was suggested that deep Pacific Ocean is isolated from the upper one at the boundary around 2000 m [*Matsumoto et al*., 2002; *Keigwin*, 1998]. In addition, on the basis of the $\delta^{13}C$ record obtained from benthic foraminifera in cores from the subarctic region, there is no evidence for enhanced NPDW formation during the glacial period [*Max et al*., 2014]. In agreement with the seawater εNd record of core MD05-2904, all of these observations suggest that deep water formation in the North Pacific (NPDW) during the LGM was probably no greater than it is today.

Numerous studies have shown that, during the last glacial period, a slowdown of the NADW formation occurred which is associated with a reduction in its propagation to the South Atlantic [*Oppo and Fairbanks*, 1987; *Duplessy et al*., 1988; *Labeyrie et al*., 1996; *Curry and Oppo*, 2005]. Benthic-planktonic foraminifera ^{14}C age difference in the North Atlantic increased greatly in the last glacial period compared to the present suggesting a decreased ventilation rate or changes in the proportions of northern-sourced water (NSW) and southern-sourced water (SSW) [*Keigwin and Schlegel*, 2002; *Keigwin*, 2004; *Robinson et al*., 2005]. Furthermore, deep water εNd values obtained from the Atlantic Ocean and the Southern Ocean for the last glacial period are characterized by more radiogenic values than the Holocene implying a higher proportion of southern-sourced water (SSW) relative to northern-sourced water (NSW) [*Rutberg et al*., 2000; *Piotrowski et al*., 2004, 2005, 2012; *Robinson and van de Flierdt*, 2009; *Roberts et al*., 2010; *Skinner et al*., 2013; *Böhm et al*., 2015]. Despite the poor level of documentation regarding past seawater changes in the Indian and Pacific Oceans, available studies indicate an enhanced northward propagation of the SSW during glacial periods [*Piotrowski et al*., 2009; *Basak et al*., 2010; *Pena et al*., 2013]. Studies undertaken on sediment cores from the equatorial Indian Ocean show positive excursions of past seawater εNd values, associated with lower $\delta^{13}C$, during glacial periods [*Piotrowski et al*., 2009; *Wilson et al*., 2012] suggesting more pronounced northward intrusion of SSW. The seawater εNd record obtained from core MD05-2904 confirms the presence of a higher proportion of SSW in the western subtropical Pacific during the last glacial period than during the late Holocene. However, this higher contribution of the CDW need to be confirmed by further investigation permitting to establish the seawater εNd record of the western equatorial Pacific (south

Philippine Sea) in order to constrain for the western Pacific Ocean the North-South Nd isotopic gradient of the CDW during glacial time.

6. Conclusion

Neodymium isotopic compositions (εNd) extracted from cleaned and uncleaned benthic and planktonic foraminifera, and Fe-Mn coatings precipitated on sediments, have been investigated for the first time in the SCS. The results are compared to modern seawater εNd to (i) assess the reliability of extraction of past seawater εNd from such an archive and to (ii) establish past circulation changes in deep water masses in the western subtropical Pacific over the past 25 kyr.

PAAS-normalized REE patterns, Mn/Ca, and Nd/Ca ratios obtained from reductively/non-reductively cleaned foraminifera and reductive cleaning solutions used for extracting Nd from associated authigenic phases in foraminifera shells reveal that the reductive cleaning process cannot remove the authigenic contaminants completely. Comparison of Nd isotopic compositions analyzed for various species of foraminiferal calcite tests and authigenic phases are quite similar and indicate that εNd obtained from cleaned and uncleaned foraminifera are overprinted by Nd deriving from authigenic Fe-Mn coatings precipitated on foraminifera. Therefore, the Nd isotopic composition of both reductively cleaned and non-reductively cleaned foraminifera reflect the bottom and/or pore water εNd and can be used as a useful tracer to reconstruct past seawater changes for deep ocean.

In contrast, the interpretation of Nd isotopic composition in bulk sediment leachates is more complicated. Although Nd isotopic composition obtained from acid-reductive HH leachates of bulk non-decarbonated sediment exhibits similar εNd values to those of foraminifera and bottom water (for core-top samples), partial dissolution of lithogenic fractions has been observed when acid-reductive HH leaching is carried out on decarbonated sediments.

The εNd record obtained from core MD05-2904 displays large variations in seawater εNd values between the LGM (-6.4 ± 0.3) and the Holocene (-4.1 ± 0.2), implying a modification of Nd inputs from rivers and/or a re-organization of the circulation in the western subtropical Pacific. The first hypothesis is not supported by the distribution of seawater εNd obtained in the northern part of the SCS [*Wu et al.*, in press]. However, further investigations, based on a high time resolution εNd record, need to be carried out in future in order to assess any potential impacts of sea level and Asian monsoon rainfall variations on sediments transfer to the deep basin of the SCS and the Nd budget of the SCS. We have proposed that these variations reflect a modification of the relative proportions of the NSW (εNd around −4) and the SSW (εNd around −8) due to vertical mixing in the Philippine Sea. The unradiogenic glacial seawater εNd values obtained in core MD05-2904 could imply a slowdown of NPDW (and NPIW) ventilation and/or a higher propagation of the CDW to the north compared to the late Holocene (last 6 kyr) (Figure 5). This interpretation imply to hypothesis that glacial CDW have not be fully modified by boundary exchange or exchange with volcanic particulates from volcanic arc of the western Pacific margin. Further analysis of εNd values of deep water masses from the southern part of the Philippine Sea and on marine core from the western subtropical Pacific needs to be realized to better constrain the Nd isotopic composition of the CDW at present time and during the last glacial period.

Acknowledgments

We would like to thank the captain, officers, and crew of R/V Marion-Dufresne for their cooperation in collecting sediment cores during the MARCO POLO cruise of the International Marine Past Global Change Study (IMAGES) program in 2005. The two anonymous reviewers are also thanked for their constructive comments on the manuscript. This work was supported by the French-Chinese International Associated Laboratories (LIA) project MONOCL, the "Agence Nationale de la Recherche" through the project MONOPOL and the ANR-10-LABX-18-01. This is LSCE contribution n°5582. All data of this study are reported in Tables 1 and 2 of the manuscript.

References

Alibo, D. S., and Y. Nozaki (2000), Dissolved rare earth elements in the South China Sea: Geochemical characterization of the water masses, *J. Geophys. Res.*, *105*, 28,771–28,783.

Amakawa, H., D. S. Alibo, and Y. Nozaki (2000), Nd isotopic composition and REE pattern in the surface waters of the eastern Indian Ocean and its adjacent seas, *Geochim. Cosmochim. Acta*, *64*, 1715–1727.

Amakawa, H., Y. Nozaki, D. S. Alibo, J. Zhang, K. Fukugawa, and H. Nagai (2004), Neodymium isotopic variations in Northwest Pacific water, *Geochim. Cosmochim. Acta*, *68*, 715–727.

Amakawa, H., K. Sasaki, and M. Ebihara (2009), Nd isotopic composition in the central North Pacific, *Geochim. Cosmochim. Acta*, *73*, 4705–4719.

Amakawa, H., H. Tazoe, H. Obata, T. Gamo, Y. Sano, and C. C. Shen (2013), Neodymium isotopic composition and concentration in the Southwest Pacific Ocean, *Geochem. J.*, *47*, 409–422.

Basak, C., E. E. Martin, K. Horikawa, and T. M. Marchitto (2010), Southern Ocean source of 14C-depleted carbon in the North Pacific Ocean during the last deglaciation, *Nat. Geosci.*, *3*(11), 770–773.

Basak, C., K. Pahnke, M. Frank, F. Lamy, and R. Gersonde (2015), Neodymium isotopic characterization of Ross Sea Bottom Water and its advection through the southern South Pacific, *Earth Planet. Sci. Lett.*, *419*, 211–221.

Bau, M., and A. Koschinsky (2009), Oxidative scavenging of cerium on hydrous Fe oxide: Evidence from the distribution of rare earth elements and yttrium between Fe oxides and Mn oxides in hydrogenetic ferromanganese crusts, *Geochem. J.*, *43*, 37–47.
Bayon, G., C. R. German, R. M. Boella, J. A. Milton, R. N. Taylor, and R. W. Nesbitt (2002), Sr and Nd isotope analyses in paleoceanography: The separation of both detrital and Fe–Mn fractions from marine sediments by sequential leaching, *Chem. Geol.*, *187*, 179–199.
Bayon, G., C. R. German, K. W. Burton, R. W. Nesbitt, and N. Rogers (2004), Sedimentary Fe–Mn oxyhydroxides as paleoceanographic archives and the role of aeolian flux in regulating oceanic dissolved REE, *Earth Planet. Sci. Lett.*, *224*, 477–492.
Bayon, G., D. Birot, L. Ruffine, J. C. Caprais, E. Ponzevera, C. Bollinger, J. P. Donval, J. L. Charlou, M. Voisset, and S. Grimaud (2011), Evidence for intense REE scavenging at cold seeps from the Niger Delta Margin, *Earth Planet. Sci. Lett.*, *312*, 443–452.
Böhm, E., J. Lippold, M. Gutjahr, M. Frank, P. Blaser, B. Antz, J. Fohlmeister, N. Frank, M. B. Andersen, and M. Deininger (2015), Strong and deep Atlantic meridional overturning circulation during the last glacial cycle, *Nature*, *517*, 73–76.
Boulay, S., C. Colin, A. Trentesaux, N. Frank, and Z. Liu (2005), Sediment sources and East Asian monsoon intensity over the last 450 ky: Mineralogical and geochemical investigations on South China Sea sediments, *Palaeogeogr. Palaeoclimatol. Palaeoecol.*, *228*, 260–277.
Bourdin, C., E. Douville, and D. Genty (2011), Alkaline-earth metal and rare-earth element incorporation control by ionic radius and growth rate on a stalagmite from the Chauvet Cave, Southeastern France, *Chem. Geol.*, *290*, 1–11.
Boyle, E. A. (1983), Manganese carbonate overgrowths on foraminifera tests, *Geochim. Cosmochim. Acta*, *47*, 1815–1819, doi:10.1016/0016-7037(83)90029-7.
Broecker, W. S., and G. H. Denton (1990), The role of ocean–atmosphere reorganizations in glacial cycles, *Quat. Sci. Rev.*, *9*, 305–341.
Carter, P., D. Vance, C. D. Hillenbrand, J. A. Smith, and D. R. Shoosmith (2012), The neodymium isotopic composition of waters masses in the eastern Pacific sector of the Southern Ocean, *Geochim. Cosmochim. Acta*, *79*, 41–59.
Chang, Y.-T., W.-L. Hsu, J.-H. Tai, T. Y. Tang, M.-H. Chang, and S.-Y. Chao (2010), Cold deep water in the South China Sea, *J. Oceanogr.*, *66*, 183–190.
Chen, C.-T., and M. Huang (1996), A mid-depth front separating the South China Sea water and the Philippine Sea water, *J. Oceanogr.*, *52*, 17−52.
Chen, C.-T., S. L. Wang, B. J. Wang, and S. C. Pai (2001), Nutrient budgets for the South China Sea basin, *Mar. Chem.*, *75*, 281–300.
Chikamoto, M. O., L. Menviel, A. Abe-Ouchi, R. Ohgaito, A. Timmermann, Y. Okazaki, A. Harada, N. AkiraOka, and A. Mouchet (2012), Variability in North Pacific intermediate and deep water ventilation during Heinrich events in two coupled climate models, *Deep Sea Res., Part II*, *61–64*, 114–126.
Copard, K., C. Colin, E. Douville, A. Freiwald, G. Gudmundsson, B. de Mol, and N. Frank (2010), Nd isotopes in deep-sea corals in the Northeastern Atlantic, *Quat. Sci. Rev.*, *29*, 2499–2508.
Curry, W. B., and D. W. Oppo (2005), Glacial water mass geometry and the distribution of ^{13}C of ΣCO_2 in the western Atlantic Ocean, *Paleoceanography*, *20*, PA1017, doi:10.1029/2004PA001021.
Duplessy, J. C., N. J. Shackleton, R. G. Fairbanks, L. Labeyrie, D. Oppo, and N. Kallel (1988), Deep water source variations during the last climatic cycle and their impact on the global deep water circulation, *Paleoceanography*, *3*, 343–360.
Elderfield, H., and E. R. Sholkovitz (1987), Rare earth elements in the pore waters of reducing nearshore sediments, *Earth Planet. Sci. Lett.*, *82*, 280–288.
Elderfield, H., R. Upstill-Goddard, and E. R. Sholkovitz (1990), The rare earth elements in rivers, estuaries, and coastal seas and their significance to the composition of ocean waters, *Geochim. Cosmochim. Acta*, *54*, 971–991.
Elmore, A. C., A. M. Piotrowski, J. D. Wright, and A. E. Scrivner (2011), Testing the extraction of past seawater Nd isotopic composition from North Atlantic deep sea sediments and foraminifera, *Geochem. Geophys. Geosyst.*, *12*, Q09008, doi:10.1029/2011GC003741.
Fang, G. H., W. D. Fang, Y. Fang, and K. Wang (1998), A survey of studies on the South China Sea upper ocean circulation, *Acta Oceanogr. Taiwan.*, *37*, 1–16.
Frank, M. (2002), Radiogenic isotopes: Tracers of past ocean circulation and erosional input, *Rev. Geophys.*, *40*(1), 1001, doi:10.1029/2000RG000094.
Galbraith, E. D., S. L. Jaccard, T. F. Pedersen, D. Sigman, G. H. Haug, M. Cook, J. Southon, and R. Francois (2007), Carbon dioxide release from the North Pacific abyss during the last deglaciation, *Nature*, *449*, 890–893.
Ge, H., Q. Li, X. Cheng, H. Zheng, and J. He (2010), Late Quaternary high resolution monsoon records in planktonic stable isotopes from northern South China Sea [in Chinese], *Earth Sci. J. China Univ. Geosci.*, *35*, 515–525, doi:10.3799/dqkx.2010.067.
Goldstein, S. L., and S. R. Hemming (2003), Long-lived isotopic tracers in oceanography, paleoceanography and ice sheet dynamics, in edited by H. D. Holland, and K. K. Turekian, Treatise on Geochemistry, vol. 6, pp. 453–489, Elsevier, Oxford, U. K.
Gong, G. C., K. K. Liu, C. T. Liu, and S. C. Pai (1992), The chemical hydrography of the South China Sea west of Luzon and a comparison with the West Philippine Sea, *Terr. Atmos. Oceanic Sci.*, *3*, 587–602.
Grenier, M., C. Jeandel, F. Lacan, D. Vance, C. Venchiarutti, A. Cros, and S. Cravatte (2013), From the subtropics to the central equatorial Pacific Ocean: Neodymium isotopic composition and rare earth element concentration variations, *J. Geophys. Res. Oceans*, *118*, 592–618, doi:10.1029/2012JC008239.
Gutjahr, M., M. Frank, C. H. Stirling, V. Klemm, T. van de Flierdt, and A. N. Halliday (2007), Reliable extraction of a deep water trace metal isotope signal from Fe–Mn oxyhydroxide coatings of marine sediments, *Chem. Geol.*, *242*, 351–370.
Gutjahr, M., M. Frank, C. H. Stirling, L. D. Keigwin, and A. N. Halliday (2008), Tracing the Nd isotope evolution of North Atlantic Deep and Intermediate Waters in the western North Atlantic since the Last Glacial Maximum from Blake Ridge sediments, *Earth Planet. Sci. Lett.*, *266*, 61–77.
Haley, B. A., G. P. Klinkhammer, and J. McManus (2004), Rare earth elements in pore waters of marine sediments, *Geochim. Cosmochim. Acta*, *68*, 1265–1279.
Haley, B. A., G. P. Klinkhammer, and A. C. Mix (2005), Revisiting the rare earth elements in foraminiferal tests, *Earth Planet. Sci. Lett.*, *239*, 79–97.
Hannigan, R. E., and E. R. Sholkovitz (2001), The development of middle rare earth element enrichments in freshwaters: Weathering of phosphate minerals, *Chem. Geol.*, *175*, 495–508.
Herguera, J. C., T. Herbert, M. Kashgarian, and C. Charles (2010), Intermediate and deep water mass distribution in the Pacific during the Last Glacial Maximum inferred from oxygen and carbon stable isotopes, *Quat. Sci. Rev.*, *29*, 1228–1245.
Horikawa, K., Y. Asahara, K. Yamamoto, and Y. Okazaki (2010), Intermediate water formation in the Bering Sea during glacial periods: Evidence from neodymium isotope ratios, *Geology*, *38*, 435–438.
Hu, D., P. Böning, C. M. Köhler, S. Hillier, N. Pressling, S. Wan, H. J. Brumsack, and P. D. Clift (2012), Deep sea records of the continental weathering and erosion response to East Asian monsoon intensification since 14 ka in the South China Sea, *Chem. Geol.*, *326–327*, 1–18.
Huang, K.-F., C.-F. You, C.-H. Chung, Y.-H. Lin, and Z. Liu (2013), Tracing the Nd isotope evolution of North Pacific Intermediate and Deep Waters through the last deglaciation from South China Sea sediments, *J. Asian Earth Sci.*, *79*, 564–573.

Jaccard, S. L., and E. D. Galbraith (2013), Direct ventilation of the North Pacific did not reach the deep ocean during the last deglaciation, *Geophys. Res. Lett.*, *40*, 199–203, doi:10.1029/2012GL054118.
Jacobsen, S. B., and G. J. Wasserburg (1980), Sm-Nd isotopic evolution of chondrites, *Earth Planet. Sci. Lett.*, *50*, 139–155.
Jeandel, C. (1993), Concentration and isotopic composition of Nd in the South Atlantic Ocean, *Earth Planet. Sci. Lett.*, *117*, 581–591.
Jeandel, C., and E. H. Oelkers (2015), The influence of terrigenous particulate material dissolution on ocean chemistry and global element cycles, *Chem. Geol.*, *395*, 50–66.
Jeandel, C., H. Delattre, M. Grenier, C. Pradoux, and F. Lacan (2013), Rare earth element concentrations and Nd isotopes in the Southeast Pacific Ocean, *Geochem. Geophys. Geosyst.*, *14*, 328–341, doi:10.1029/2012GC004309.
Kawabe, M., and S. Fujio (2010), Pacific Ocean circulation based on observation, *J. Oceanogr.*, *66*, 389–403.
Kawabe, M., S. Fujio, and D. Yanagimoto (2003), Deep-water circulation at low latitudes in the western North Pacific, *Deep Sea Res., Part I*, *50*, 631–656.
Kawabe, M., D. Yanagimoto, S. Kitagawa, and Y. Kuroda (2005), Variations of the deep western boundary current in Wake Island Passage, *Deep Sea Res., Part I*, *52*, 1121–1137.
Kawabe, M., D. Yanagimoto, and S. Kitagawa (2006), Variations of deep western boundary currents in the Melanesian Basin in the western North Pacific, *Deep Sea Res., Part I*, *53*, 942–959.
Kawabe, M., S. Fujio, D. Yanagimoto, and K. Tanaka (2009), Water masses and currents of deep circulation southwest of the Shatsky Rise in the western North Pacific, *Deep Sea Res., Part I*, *56*, 1675–1687.
Keigwin, L. D. (1998), Glacial-age hydrography of the far northwest Pacific Ocean, *Paleoceanography*, *13*, 323–339.
Keigwin, L. D. (2004), Radiocarbon and stable isotope constraints on last glacial maximum and Younger Dryas ventilation in the western North Atlantic, *Paleoceanography*, *19*, PA4012, doi:10.1029/2004PA001029.
Keigwin, L. D., and M. A. Schlegel (2002), Ocean ventilation and sedimentation since the glacial maximum at 3 km in the western North Atlantic, *Geochem. Geophys. Geosyst.*, *3*(6), 1034, doi:10.1029/2001GC000283.
Kraft, S., M. Frank, E. C. Hathorne, and S. Weldeab (2013), Assessment of seawater Nd isotope signatures extracted from foraminiferal shells and authigenic phases of Gulf of Guinea sediments, *Geochim. Cosmochim. Acta*, *121*, 414–435.
Labeyrie, L. D., et al. (1996), Hydrographic changes of the Southern Ocean (southeast Indian sector) over the last 230 kyr, *Paleoceanography*, *11*, 57–76.
Lacan, F., and C. Jeandel (2001), Tracing Papua New Guinea imprint on the central Equatorial Pacific Ocean using neodymium isotopic compositions and rare earth element patterns, *Earth Planet. Sci. Lett.*, *186*, 497–512.
Lacan, F., and C. Jeandel (2005), Neodymium isotopes as a new tool for quantifying exchange fluxes at the continent-ocean interface, *Earth Planet. Sci. Lett.*, *232*, 245–257.
Li, L., and T. Qu (2006), Thermohaline circulation in the Deep South China Sea basin as inferred from oxygen distributions, *J. Geophys. Res.*, *111*, C05017, doi:10.1029/2005JC003164.
Liu, Z., C. Colin, W. Huang, K. P. Le, S. Tong, Z. Chen, and A. Trentesaux (2007), Climatic and tectonic controls on weathering in South China and the Indochina Peninsula: Clay mineralogical and geochemical investigations from the Pearl, Red, and Mekong drainage basins, *Geochem. Geophys. Geosyst.*, *8*, Q05005, doi:10.1029/2006GC001490.
Liu, Z., X. Li, C. Colin, and H. Ge (2010), A high-resolution clay mineralogical record in the northern South China Sea since the Last Glacial Maximum, and its time series provenance analysis, *Chin. Sci. Bull.*, *55*, 4058–4068.
Liu, Z., et al. (2015), Source-to-sink transport process of fluvial sediments in the South China Sea, *Earth Sci. Rev.*, doi:10.1016/j.earscirev.2015.08.005, in press.
Lugmair, G. W., T. Shimamura, R. S. Lewis, and E. Anders (1983), Samarium-146 in the early solar system: Evidence from neodymium in the allende meteorite, *Science*, *222*, 1015–1018.
Martin, E. E., S. W. Blair, G. D. Kamenov, H. D. Scher, E. Bourbon, C. Basak, and D. N. Newkirk (2010), Extraction of Nd isotopes from bulk deep sea sediments for paleoceanographic studies on Cenozoic time scales, *Chem. Geol.*, *269*, 414–431.
Martínez-Botí, M. A., D. Vance, and P. G. Mortyn (2009), Nd/Ca ratios in plankton-towed and core top foraminifera: Confirmation of the water column acquisition of Nd, *Geochem. Geophys. Geosyst.*, *10*, Q08018, doi:10.1029/2009GC002701.
Matsumoto, K., T. Oba, J. Lynch-Stieglitz, and H. Yamamoto (2002), Interior hydrography and circulation of the glacial Pacific Ocean, *Quat. Sci. Rev.*, *21*, 1693–1704.
Max, L., L. Lembke-Jene, J.-R. Riethdorf, R. Tiedemann, D. Nürnberg, H. Kühn, and A. Mackensen (2014), Pulses of enhanced North Pacific Intermediate Water ventilation from the Okhotsk Sea and Bering Sea during the last deglaciation, *Clim. Past*, *10*, 591–605.
Molina-Kescher, M., M. Frank, and E. Hathorne (2014a), South Pacific dissolved Nd isotope compositions and rare earth element distributions: Water mass mixing versus biogeochemical cycling, *Geochim. Cosmochim. Acta*, *127*, 171–189.
Molina-Kescher, M., M. Frank, and E. C. Hathorne (2014b), Nd and Sr isotope compositions of different phases of surface sediments in the South Pacific: Extraction of seawater signatures, boundary exchange, and detrital/dust provenance, *Geochem. Geophys. Geosyst.*, *15*, 3502–3520, doi:10.1002/2014GC005443.
Nance, W. B., and S. R. Taylor (1976), Rare-earth element patterns and crustal evolution. 1. Australian post-Archean sedimentary rocks, *Geochim. Cosmochim. Acta*, *40*, 1539–1551.
Noble, T. L., A. M. Piotrowski, and I. N. McCave (2013), Neodymium isotopic composition of intermediate and deep waters in the glacial southwest Pacific, *Earth Planet. Sci. Lett.*, *384*, 27–36.
Ohta, A., and I. Kawabe (2001), REE (III) adsorption onto Mn dioxide (δ-MnO_2) and Fe oxyhydroxide: Ce (III) oxidation by δ-MnO_2, *Geochim. Cosmochim. Acta*, *65*, 695–703.
Okazaki, Y., A. Timmermann, L. Menviel, N. Harada, A. Abe-Ouchi, M. O. Chikamoto, A. Mouchet, and H. Asahi (2010), Deepwater formation in the North Pacific during the Last Glacial Termination, *Science*, *329*, 200–204.
Oppo, D. W., and R. G. Fairbanks (1987), Variability in the deep and intermediate water circulation of the Atlantic Ocean during the past 25,000 years—Northern Hemisphere modulation of the Southern Ocean, *Earth Planet. Sci. Lett.*, *86*, 1–15.
Osborne, A. H., D. Vance, E. J. Rohling, N. Barton, M. Rogerson, and N. Fello (2008), A humid corridor across the Sahara for the migration of early modern humans out of Africa 120,000 years ago, *Proc. Natl. Acad. Sci.*, *105*, 16444–16447.
Palmer, M. R. (1985), Rare earth elements in foraminifera tests, *Earth Planet. Sci. Lett.*, *73*, 285–298.
Pena, L. D., E. Calvo, I. Cacho, S. Eggins, and C. Pelejero (2005), Identification and removal of Mn–Mg-Rich contaminant phases on foraminiferal tests: Implications for Mg/Ca past temperature reconstructions, *Geochem. Geophys. Geosyst.*, *6*, Q09P02, doi:10.1029/2005GC000930.
Pena, L. D., S. L. Goldstein, S. R. Hemming, K. M. Jones, E. Calvo, C. Pelejero, and I. Cacho (2013), Rapid changes in meridional advection of Southern Ocean intermediate waters to the tropical Pacific during the last 30 kyr, *Earth Planet. Sci. Lett.*, *368*, 20–32.

Piepgras, D. J., and S. B. Jacobsen (1988), The isotopic composition of neodymium in the North Pacific, *Geochim. Cosmochim. Acta*, *52*, 1373–1381.
Piepgras, D. J., and G. J. Wasserburg (1980), Neodymium isotopic variations in seawater, *Earth Planet. Sci. Lett.*, *50*, 128–138.
Piepgras, D. J., and G. J. Wasserburg (1982), Isotopic composition of neodymium in waters from Drake Passage, *Science*, *217*, 207−217.
Pin, C., and J. F. Santos Zalduegui (1997), Sequential separation of light rare-earth elements, thorium and uranium by miniaturized extraction chromatography: Application to isotopic analyses of silicate rocks, *Anal. Chim. Acta*, *339*, 79–89.
Piotrowski, A. M., S. L. Goldstein, S. R. Hemming, and R. G. Fairbanks (2004), Intensification and variability of ocean thermohaline circulation through the last deglaciation, *Earth Planet. Sci. Lett.*, *225*, 205–220.
Piotrowski, A. M., S. L. Goldstein, S. R. Hemming, and R. G. Fairbanks (2005), Temporal relationships of carbon cycling and ocean circulation at glacial boundaries, *Science*, *307*, 1933–1938.
Piotrowski, A. M., V. K. Banakar, A. E. Scrivner, H. Elderfield, A. Galy, and A. Dennis (2009), Indian Ocean circulation and productivity during the last glacial cycle, *Earth Planet. Sci. Lett.*, *285*, 179–189.
Piotrowski, A. M., A. Galy, J. A. L. Nicholl, N. Roberts, D. J. Wilson, J. A. Clegg, and J. Yu (2012), Reconstructing deglacial North and South Atlantic deep water sourcing using foraminiferal Nd isotopes, *Earth Planet. Sci. Lett.*, *357–358*, 289–297.
Pomiès, C., G. R. Davies, and S. M.-H. Conan (2002), Neodymium in modern foraminifera from the Indian Ocean: Implications for the use of foraminiferal Nd isotope compositions in paleooceanography, *Earth Planet. Sci. Lett.*, *203*, 1031–1045.
Qu, T. (2002), Evidence for water exchange between the South China Sea and the Pacific Ocean through the Luzon Strait, *Acta Oceanol. Sin.*, *21*, 175–185.
Qu, T., Y. Du, and H. Sasaki (2006), South China Sea throughflow: A heat and freshwater conveyor, *Geophys. Res. Lett.*, *33*, L23617, doi: 10.1029/2006GL028350.
Rae, J. W. B., M. Sarnthein, G. L. Foster, A. Ridgwell, P. M. Grootes, and T. Elliott (2014), Deep water formation in the North Pacific and deglacial CO_2 rise, *Paleoceanography*, *29*, 645–667, doi:10.1002/2013PA002570.
Rahmstorf, S. (2002), Ocean circulation and climate during the past 120,000 years, *Nature*, *419*, 207–214.
Reid, J. L. (1997), On the total geostrophic circulation of the Pacific Ocean: Flow patterns, traces and transports, *Prog. Oceanogr.*, *39*, 263–325.
Rella, S. F., and M. Uchida (2014), A Southern Ocean trigger for Northwest Pacific ventilation during the Holocene?, *Sci. Rep.*, *4*, 4046, doi: 10.1038/srep04046.
Rella, S. F., R. Tada, K. Nagashima, M. Ikehara, T. Itaki, K. Ohkushi, T. Sakamot, N. Harada, and M. Uchida (2012), Abrupt changes of intermediate water properties on the northeastern slope of the Bering Sea during the last glacial and deglacial period, *Paleoceanography*, *27*, PA3203, doi:10.1029/2011PA002205.
Rickli, J., M. Gutjahr, D. Vance, M. Fischer Gödde, C. D. Hillenbrand, and G. Kuhn (2014), Neodymium and hafnium boundary contributions to seawater along the West Antarctic continental margin, *Earth Planet. Sci. Lett.*, *394*, 99–110.
Roberts, N. L., A. M. Piotrowski, J. F. McManus, and L. D. Keigwin (2010), Synchronous deglacial overturning and water mass source changes, *Science*, *327*, 75–78.
Roberts, N. L., A. M. Piotrowski, H. Elderfield, T. I. Eglinton, and M. W. Lomas (2012), Rare earth element association with foraminifera, *Geochim. Cosmochim. Acta*, *94*, 57–71.
Robinson, L., J. F. Adkins, L. D. Keigwin, J. Southon, D. P. Fernandez, S.-L. Wang, and D. S. Scheirer (2005), Radiocarbon variability in the Western North Atlantic during the last deglaciation, *Science*, *310*, 1469–1473.
Robinson, L. F., and T. van de Flierdt (2009), Southern Ocean evidence for reduced export of North Atlantic Deep Water during Heinrich event 1, *Geology*, *37*, 195–198.
Rutberg, R. L., S. R. Hemming, and S. L. Goldstein (2000), Reduced North Atlantic Deep Water flux to the glacial Southern Ocean inferred from neodymium isotope ratios, *Nature*, *405*, 935–938.
Shaw, P. T., and S. Y. Chao (1994), Surface circulation in the South China Sea, *Deep Sea Res., Part I*, *41*, 1663–1683.
Siedler, G., J. Holfort, W. Zenk, T. J. Müller, and T. Csernok (2004), Deep-water flow in the Mariana and Caroline basins, *J. Phys. Oceanogr.*, *34*, 566–581.
Skinner, L. C., A. E. Scrivner, D. Vance, S. Barker, S. Fallon, and C. Waelbroeck (2013), North Atlantic versus Southern Ocean contributions to a deglacial surge in deep ocean ventilation, *Geology*, *4*, 667–670.
Stichel, T., M. Frank, J. Rickli, and B. A. Haley (2012), The hafnium and neodymium isotope composition of seawater in the Atlantic sector of the Southern Ocean, *Earth Planet. Sci. Lett.*, *317–318*, 282–294.
Surya Prakash, L., et al. (2012), Distribution of REES and yttrium among major geochemical phases of marine Fe–Mn-oxides: Comparative study between hydrogenous and hydrothermal deposits, *Chem. Geol.*, *312–313*, 127–137.
Tachikawa, K., T. Toyofuku, I. Basile-Doelsch, and T. Delhaye (2013), Microscale neodymium distribution in sedimentary planktonic foraminiferal tests and associated mineral phases, *Geochim. Cosmochim. Acta*, *100*, 11–23.
Tachikawa, K., A. M. Piotrowski, and G. Bayon (2014), Neodymium associated with foraminiferal carbonate as a recorder of seawater isotopic signatures, *Quat. Sci. Rev.*, *88*, 1–13.
Talley, D., and J.-Y. Yun (2001), The role of cabbeling and double diffusion in setting the density of the North Pacific Intermediate Water salinity minimum, *J. Phys. Oceanogr.*, *31*, 1538–1549.
Talley, L. D., and T. M. Joyce (1992), The double silica maximum in the North Pacific, *J. Geophys. Res.*, *97*, 5465–5480.
Tanaka, T., et al. (2000), JNdi-1: A neodymium isotopic reference in consistency with La Jolla neodymium, *Chem. Geol.*, *168*, 279–281.
Tian, J., Q. Yang, X. Liang, D. Hu, F. Wang, and T. Qu (2006), The observation of Luzon strait transport, *Geophys. Res. Lett.*, *33*, L19607, doi: 10.1029/2006GL026272.
Tian, J., Q. Yang, and W. Zhao (2009), Observation of enhanced diapycnal mixing in the South China Sea, *J. Phys. Oceanogr.*, *39*, 3191–3203.
Vance, D., and K. Burton (1999), Neodymium isotopes in planktonic foraminifera: A record of the response of continental weathering and ocean circulation rates to climate change, *Earth Planet. Sci. Lett.*, *173*, 365–379.
Vance, D., A. E. Scrivner, P. Beney, M. Staubwasser, G. M. Henderson, and N. C. Slowey (2004), The use of foraminifera as a record of the past neodymium isotope composition of seawater, *Paleoceanography*, *19*, PA2009, doi:10.1029/2003PA000957.
Wan, S., and Z. Jian (2014), Deep water exchanges between the South China Sea and the Pacific since the last glacial period, *Paleoceanography*, *29*, 1162–1178, doi:10.1002/2013PA002578.
Wang, G., S.-P. Xie, T. Qu, and R. X. Huang (2011), Deep South China Sea circulation, *Geophys. Res. Lett.*, *38*, L05601, doi:10.1029/2010GL046626.

Wei, G. J., Y. Liu, J. L. Ma, L. H. Xie, J. F. Chen, W. F. Deng, and S. Tang (2012), Nd, Sr isotopes and elemental geochemistry of surface sediments from the South China Sea: Implications for Provenance Tracing, *Mar. Geol.*, *319–322*, 21–34.

Wilson, D. J., A. M. Piotrowski, A. Galy, and J. A. Clegg (2013), Reactivity of neodymium carriers in deep sea sediments: Implications for boundary exchange and paleoceanography, *Geochim. Cosmochim. Acta*, *109*, 197–221.

Wilson, D. J., A. M. Piotrowski, A. Galy, and I. N. McCave (2012), A boundary exchange influence on deglacial neodymium isotope records from the deep western Indian Ocean, *Earth Planet. Sci. Lett.*, *341–344*, 35–47.

Wu, Q., C. Colin, Z. Liu, F. Thil, E. Douville, Q. Dubois-Dauphin, and N. Frank, New insights into hydrological exchange between the South China Sea and the western Pacific Ocean based on the Nd isotopic composition of seawater, Deep-Sea Research II, the South China Sea Deep Special Issue, in press.

Wyrtki, K. (1961), Physical oceanography of the Southeast Asian waters, *Naga Rep. 2*, 195 pp., Scripps Inst. of Oceanogr., La Jolla, Calif.

Xie, L., J. Tian, S. Zhang, Y. Zhang, and Q. Yang (2011), An anticyclonic eddy in the intermediate layer of the Luzon Strait in Autumn 2005, *J. Oceanogr.*, *67*, 37–46.

Yang, Q., J. Tian, and W. Zhao (2010), Observation of Luzon Strait transport in Summer 2007, *Deep Sea Res., Part I*, *57*, 670–676.

Zenk, W., G. Siedler, A. Ishida, J. Holfort, Y. Kashino, Y. Kuroda, T. Miyama, and T. J. Müller (2005), Pathways and variability of the Antarctic Intermediate Water in the western equatorial Pacific Ocean, *Prog. Oceanogr.*, *67*, 245–281.

Zhao, W., C. Zhou, J. Tian, Q. Yang, B. Wang, L. Xie, and T. Qu (2014), Deep water circulation in the Luzon Strait, *J. Geophys. Res. Occens*, *119*, 790–804, doi:10.1002/2013JC009587.

Zweng, M. M, et al. (2013), World Ocean Atlas 2013, Volume 2: Salinity, edited by S. Levitus, and A. Mishonov Technical Ed.; NOAA Atlas NESDIS 74, 39 pp.